A STUDY OF FLUX QUANTIZATION

R. Meservey

Final Technical Report
31 March, 1970

Prepared under Contract No. NAS-12-101 by the
FRANCIS BITTER NATIONAL MAGNET LABORATORY
Massachusetts Institute of Technology
Cambridge, Massachusetts

Sponsored by

Electronics Research Center

NATIONAL AERONAUTICS AND SPACE ADMINISTRATION

CONTENTS

A STUDY OF FLUX QUANTIZATION

By R. Meservey

Francis Bitter National Magnet Laboratory
Massachusetts Institute of Technology
Cambridge, Massachusetts

SUMMARY

This research was concerned with the study of flux quantization in superconductors. The investigation consisted of basic measurements of the phenomena of flux quantization as well as feasibility studies of potential applications. A vacuum evaporation laboratory was set up to produce the required thin-film geometries. An extensive study was undertaken of flux quantization effects in thin film microcylinders (diameter $\approx$ .5 to 5 microns) of indium and aluminum (340 Å to 2000 Å thick). The phase boundary was measured in a parallel magnetic field and as a function of the field angle. The results agree in most respects with theoretical predictions. A search for higher order correlations in superconductors gave a negative result. The effect of fluctuations was probably observed. A flux quantization magnetometer and prototype ammeter were built to determine the feasibility of such instruments. The magnetometer could detect 10^{-8} gauss, but it was concluded that a thin film bridge detector design was essential for reproducible operation. With the ammeter it was concluded that with very careful design and calibration such an instrument could measure a a current or a magnetic field in terms of the standard length and the constant h/2e to an accuracy approaching one part in 10^{6}. Measurements were made of the absolute value of the penetration depth in thin films of Sn and Pb. The temperature dependence of the penetration depth of aluminum was measured with a pure annealed aluminum wire and found not to agree closely with the value predicted by the BCS theory. The kinetic inductance was measured quantitatively for the first time in thin films and wires of Sn and found to agree rather accurately with theoretical predictions. Very sensitive transducers of temperature, magnetic field, and current density were developed using a digital inductance meter. This inductance meter was also used with a paramagnetic salt to give a digital thermometer.

List of Symbols

A = vector potential

B = magnetic induction

C = capacitance

d = thickness of microcylinder

δ = thickness of insulator in rectangular superconducting loop

E = electric field

H = magnetic field

H_o = magnetic field applied parallel to surface of superconductor

H_c = superconducting critical field

H_{cb} = critical field of bulk superconductor

Δ H = Field period of flux quantization

h = Planck's constant

Hz = hertz

I = electric current

J = current density

L = characteristic length

L = inductance

L_M = magnetic inductance

L_K = kinetic inductance

ℓ = length of conductor

$\Lambda = m/ne^2$

λ = superconducting penetration depth

m = mass of an electron

μ = permeability

N = quantum number

n = carrier concentration

ν = frequency

P_s = momentum of supercarrier

Φ = magnetic flux

Φ_o = h/2e = quantum of flux

$Q = \omega L/R$ = "Q"; resonant circuit

R = radius of microcylinder

List of Symbols (cont.)

R = resistance

R_N = resistance of normal state

σ = cross sectional area

t = temperature

T_c = superconducting transition temperature

$\Delta t_c = [T_c(0) - T_c(H)]/T_c(0)$

$t = T/T_c$

θ = Angle between axis of microcylinder and the magnetic field

t = time

τ = electronic colision time, normal state

V = voltage

v_s = velocity of supercarrier

W = width of insulator in rectangular superconducting loop

x = coordinate $\perp$ to superconducting surface

ω = angular frequency

$\Delta \omega$ = change in angular frequency of resonant circuit

INTRODUCTION

The discovery of flux quantization in superconductors was one of the important scientific discoveries of the past decade. The investigation which we are reporting here was started when it became clear that flux quantization and related phenomena in superconductors had a promising future. There was promise of important scientific discoveries and also of revolutionary technological developments. In the subsequent four years basic understanding of flux quantization phenomena and the techniques of their applications to science and technology have developed greatly. Contributions have been made by the present investigation and by a large number of other investigations. The result is that this field has been opened up, the first important applications are becoming a reality, and the potential future developments have been brought into focus. To place this report in its scientific context, a brief description of the nature of the phenomena and its historical background will be given.

Background

In 1961, Doll and Näbauer (Ref. 1) and Deaver and Fairbank (Ref. 2) independently observed that the moments produced by trapping magnetic flux in small superconducting cylinders were quantized and that the corresponding flux quanta were of magnitude $\frac{h}{2e}$ (mks units). The quantization had been predicted by London (Ref. 3) and by Onsager (Ref. 4) in units $\frac{h}{e}$. Onsager (Ref. 5) quickly pointed out that the factor of 2 came from the pairing of electrons as postulated by the BCS (Ref. 6) theory of superconductivity.

The quantization of flux is a corollary of the quantization of angular momentum of a closed quantum system. Although detailed understanding of why metals are superconducting involves very complex questions, the electrical behavior of superconductors follows largely from the Bohr-Sommerfeld quantum condition on the momentum of the superconducting electron pairs,

$$\oint P_s \, dl = Nh. \quad N = 0, \ 1, \ 2. \ . \ . \tag{1}$$

Since these are charged particles, they have a magnetic interaction with other moving charge carriers and the canonical momentum of the superconducting pairs, $P_s = 2mv_s + 2eA$, contains the vector potential A which accounts for these interactions so that

$$\oint (2mv_s + 2eA) \, dl = Nh. \tag{2}$$

The line integral $\oint A dl = \Phi$, the flux contained in the enclosed contour, so that,

$$\frac{m}{e} \oint v_s dl + \Phi = N \, (h/2e) \tag{3}$$

On any contour on which the first integral is 0, the flux Φ is quantized,

$$\Phi = N \, (h/2e), \ N = 0, \ 1, \ 2. \ . \ . \tag{4}$$

Quantization of angular momentum is found in all isolated quantum systems; the remarkable thing about superconductors is that this quantization is for a system of macroscopic size.

Shortly after the discovery of flux quantization two very closely related affects were predicted by Josephson (Ref. 7) for superconductors separated by a barrier through which superconducting pairs could tunnel. The dc Josephson effect is very closely related to flux quantization. The ac Josephson effect is the energy-time analog of flux quantization. This follows since the voltage is proportional to the time rate of change of flux and from equation 4,

$$V = \oint E \cdot d\ell = \frac{-d\varphi}{dt} = \frac{-dN}{dt} (h/2e) = \nu \, (h/2e). \tag{5}$$

Here the frequency ν is the rate of change of the quantum state. Thus the flux quantum $\varphi_o = \frac{h}{2e}$ comes into both the time dependent and the non-time dependent effect.

Research Objectives

The research program undertaken under contract NAS-12-101 had three main objectives.

1. Study the phenomenon of flux quantization in superconductors.
2. Measure fundemental properties of superconductors using the technique of flux quantization.
3. Investigate the feasibility of applications of flux quantization.

The emphasis of the program was principally designed to probe the basic physical questions inherent in flux quantization and the behavior of superconductors. At the same time, however, certain applications were considered so important, both to technology and as a scientific tool, that investigation of their feasibility was also a major goal.

In the continuation of the contract for the second two-year period the program followed from the original program but was considerably different in emphasis. The research under the continuing program was directed more toward applying flux quantization, measuring techniques and investigating certain new applications of thin film superconductors.

RESEARCH PROGRAM

The research program was carried over a period of four years and several persons contributed to the program. The principal investigator was Dr. R. Meservey of the staff of the Francis Bitter National Magnet Laboratory. Directly involved in major phases of the investigation were Dr. Paul Tedrow of the Magnet Laboratory, Professor L. Meyers, visiting scientist from Boston University, and Gerald Peabody, doctoral candidate at Harvard University. Contributing to the program as consultants were Lawrence Rubin, Dr. E. Maxwell, Dr. C. Chase, and Dr. Robin Oder, all of the staff of the Magnet Laboratory. The construction of equipment and preparation of samples was carried out mainly by R. MacNabb,

J. De Martino, and R. Merrican. Major phases of the research program will be described below.

Facilities and Techniques

Vacuum evaporation laboratory. -- Since much of the research involved thin films a high priority task was the setting up of the vacuum evaporation laboratory. To begin with, a very high vacuum dual purpose pumping station was assembled. This consisted of a 6 inch diffusion pump, gate valve, and cold trap and was entirely made of stainless steel and copper in the high vacuum region. The mechanical pump was separated from the diffusion pump by a zeolite trap to prevent contamination of the high vacuum diffusion pump fluid. The usual sources of cooling water in electrical power were provided with a system of safety interlocks to prevent damage to the system from failure of water pressure, power, or components of the system. For thin film evaporations two separate evaporation units were assembled to fit on the base of this pumping station. The evaporation units were each mounted on separate vacuum collars and either unit could be placed on the base plate of the pumping station. Fig. 1 shows a general view of the laboratory with the main evaporation unit in place and two auxiliary evaporation units.

The main evaporation unit, which is shown in Fig. 2, consisted of an Allen-Jones Carousel mask changer mounted on a 18" collar with an 18" glass bell jar. The system was constructed of stainless steel, copper, and glass and viton O-rings and gaskets. A bakeout canopy was provided and the whole system designed to be baked out at 150°C. The mask changing unit (Fig. 3) had 6 evaporation sources, 6 mask holders, and 6 substrate holders (2"x2"). Any one of these sources, masks or substrates could be located in the evaporation position in any order. This allowed the building up of complex thin film structures by successive evaporations without breaking vacuum. The 18" evaporation unit reached a vacuum of 3×10^{-8} torr without bakeout. With an over-night bakeout and liquid nitrogen trapping a vacuum of 5×10^{-9} torr could be reached. A glow discharge system was installed for cleaning substrates and forming oxide layers on metal films.

Fig. 1 General view of vacuum evaporation laboratory.

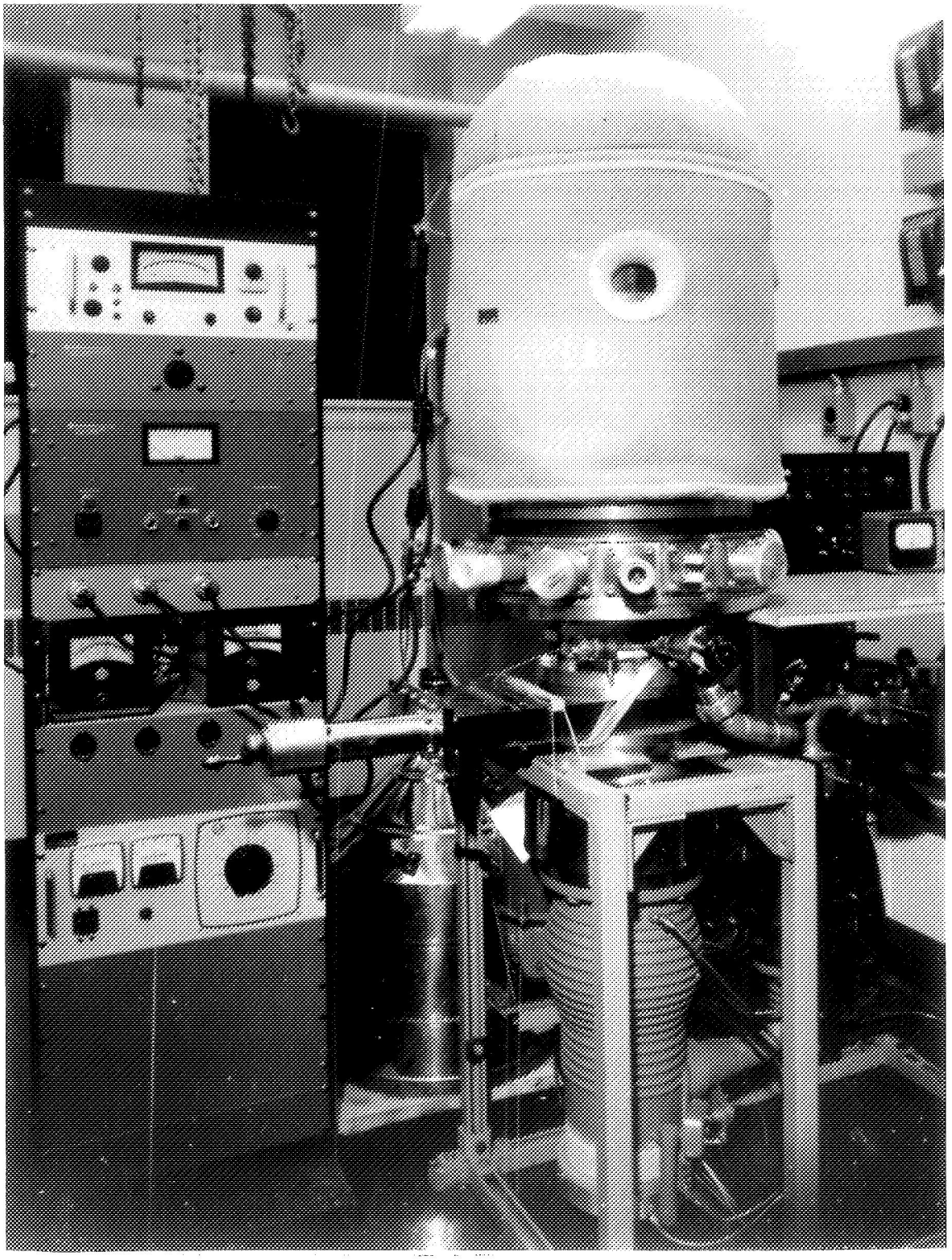

Fig. 2 Very high vacuum pumping station with 18" evaporation system.

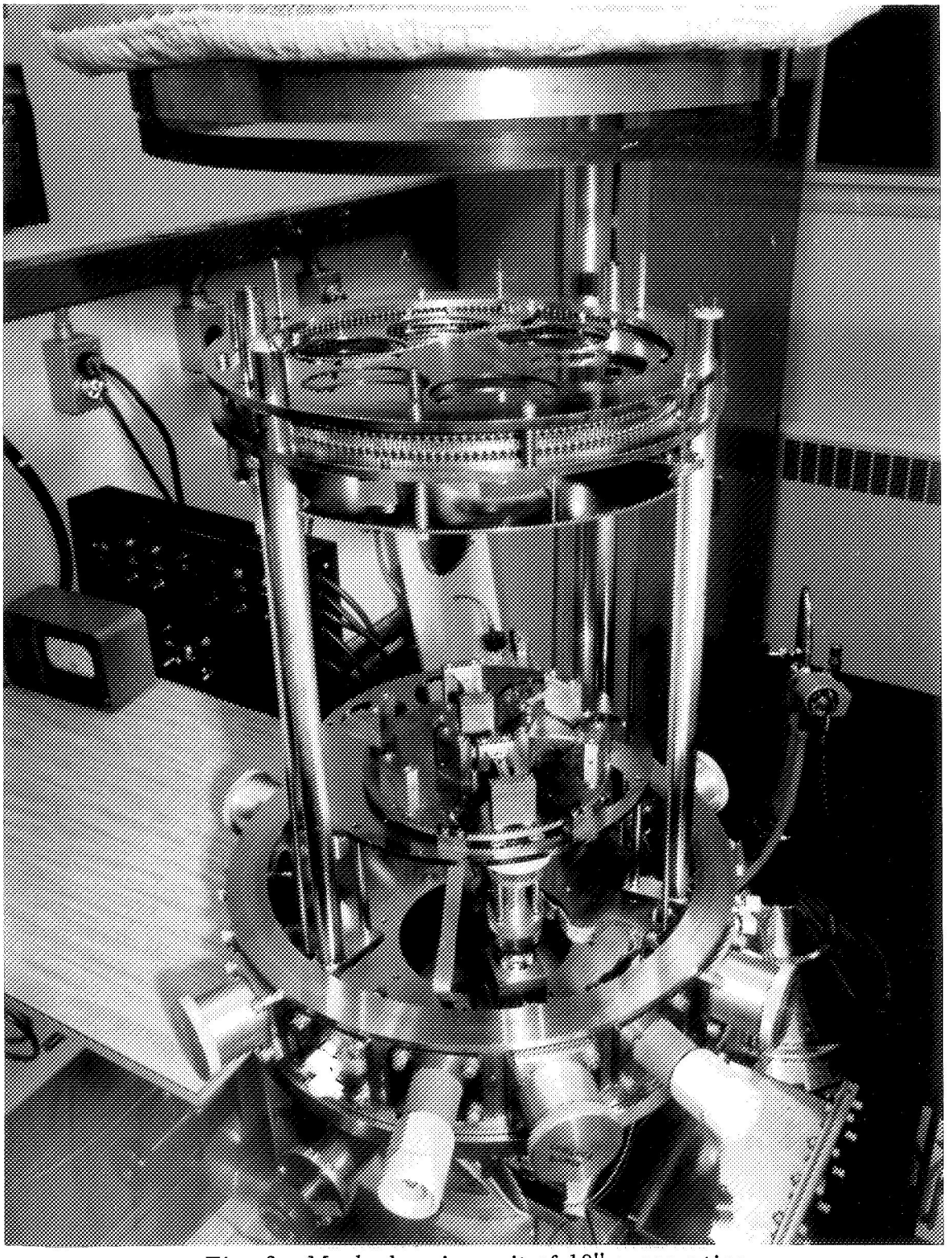

Fig. 3 Mask changing unit of 18" evaporation system.

A special substrate cooling mechanism was designed so that both substrates and masks could be changed and then cooled to liquid nitrogen temperature without breaking vacuum.

The second evaporation unit which could be substituted for the 18" system on the pumping station consisted of a 12" stainless steel collar glass bell jar. This system allowed evaporation on rotating cylindrical substrates and also had a simple cylindrical masking device. This system also had a liquid helium cold trap for cryopumping to very low pressures and was provided with an electron beam source for evaporation of refractory materials.

In the latter part of the research program, a radio frequency sputtering equipment was procured from Materials Research Corp. and was used for sputtering dielectrics for insulating layers, or sputtering refractory metals such as niobium, and for sputter etching of thin film circuits.

In addition to these main facilities, the vacuum evaporation laboratory contained considerable auxiliary equipment. A second evaporation system, which operated in the region of 10^{-6} torr was built for routine work not requiring very high vacuum or the mask changer. A Sloan vibrating crystal thickness monitor was used to control the thickness of the evaporation. The exact final thickness was measured with a Hilger multiple beam interference instrument. Facilities for substrate cleaning were provided. A spinner was used to coat thin film samples with photo-resist which could then be exposed in a simple optical system using photographic masks to provide the desired thin film patterns.

Cryogenic facility. -- The low temperature measurements were all made in one of two glass dewar systems, which were pumped by a mechanical pump and, if needed, a six-inch Stokes booster diffusion pump capable of reducing the temperature of the liquid helium to a temperature of 0.87°K. The temperature was determined from vapor pressure measurements made on mercury and oil manometers, Wallace and Tiernan dial gauges, and an MKS Baratron pressure gauge, together with carbon resistance thermometers whose resistance was measured in

a 33 cycle bridge. This bridge and a temperature control unit (Ref. 8) was used to regulate the temperature to a few micro-degrees in the lower temperature region.

The glass dewar systems could be surrounded by three Molypermalloy cylindrical magnetic shields approximately three feet long and ranging from 6 inches to 8 inches inside diameter. These shields,which were 1/16 inch thick, were separately wound with toroidal demagnetization coils so that they could be demagnetized separately and in sequence. This system of shielding reduced the ambient field near the center of the cylinders to about 10^{-4} gauss. For magnetic field measurements a copper solenoid with compensating end coils to give a very uniform field near the center of the solenoid could be placed on the outside of the liquid helium dewar held snugly with berrylium copper springs and operating in the liquid nitrogen bath. This magnet, which was used mainly for measurements of the effect of magnetic field on thin film microcylinders, could give up to about 400 gauss. In addition, a superconducting magnet with a 2 inch inside diameter was constructed by the Magnet Design Group of the National Magnet Laboratory to give a field of up to 20,000 gauss. This magnet was capable of locked-in superconducting mode, a field of which could be swept over a limited range by an auxiliary coil.

Flux Quantization in Microcylinders

Shortly after the initial discovery of flux quantization, Little and Parks (Ref. 9) made the discovery that the transition temperature of very small superconducting cylinders (designated here microcylinders) was periodic with a magnetic field applied parallel to the axis of the cylinder. This periodicity in transition temperature was found to correspond to fields which gave integral values of the flux quantum through the microcylinder, whose diameter was the order of microns.

This type of experiment has several advantages for studying the basic phenomena of flux quantization. The geometry is the simplest possible for a doubly-

connected system. A rather complete theory of this effect based on the Ginzburg-Landau (Ref. 10) equations has been given by Tinkham (Ref. 11). Because we are only concerned with the normal-superconducting state phase boundary, the form of the theory is simple and rigorous. The very small area of these microcylinders means that the field corresponding to one flux quantum is comparatively large, being typically 0.1 - 10 gauss, and the amplitude of the voltage oscillations actually measured is also large because of the small size of the cylinders. These three facts make this type of experiment very useful in understanding and measuring basic effects in flux quantization.

The present investigation extended the range of quantitative measurements on aluminum microcylinders to thinner films and larger diameters and gives some results on indium. These are the first measurements in which the magnetic field has been accurately aligned with the axis of the microcylinders. This is very important, particularly in cylinders of large diameter. Measurements have also been made of the effect of a magnetic field at angles other than parallel to the direction of the axis of the cylinder. Observations were made of the fine structure of the phase boundary and of the probable presence of fluctuation phenomena. A search was made for higher order correlations, that is for evidence that there is not only pairing of electrons but some grouping of electrons in fours, sixes, eights, and etc. The techniques used and the results of these measurements is being reported in detail in two articles which are being prepared for publication. What follows is a short condensation of some of these results.

Theory. -- The basic results of the Tinkham theory (Ref. 11) is that the phase boundary between the normal and superconducting state of thin film cylinder is given by the following expression for H_c and T_c (H).

$$T_c(H) = T_c(0)\left\{1 - \frac{R^2}{8\lambda^2(0)H_{cB}^2(0)}\left[\left(H\cos\theta - \frac{n\phi}{\pi R^2}\right)^2 + \frac{1}{3}\frac{d^2}{R^2}H^2\cos^2\theta + 4H^2\sin^2\theta\right]\right\} \quad (6)$$

In this expression $T_c(H)$ is the critical temperature for an applied magnetic field, H. $T_c(0)$ is the critical temperature for H = 0 and R is the mean radius of the cylinder, whose thickness d is assumed to be small compared with R. The angle θ is that measured between the direction H and the axis of the cylinder. Eq. 6 is derived assuming the standard temperature dependencies for the penetration depth and the critical fields.

$$\lambda(t) = \lambda(0)\left[1-t^4\right]^{-1/2} \tag{7}$$

$$H_{cb}(t) = H_{cb}(0)\left[1-t^2\right] \tag{8}$$

Where $\lambda(0)$ and $H_{cb}(0)$ are the penetration depth and the bulk critical field at T = 0.

In the case where $\theta = 0$, Eq. 7 becomes

$$\Delta t_c = \frac{T_c(0) - T_c(H)}{T_c(0)} = \frac{R^2}{8\lambda^2(0)\,H_{cb}^2(0)}\left\{\left(H - \frac{n\Phi_0}{\pi R^2}\right)^2 + \frac{1}{3}\frac{d^2}{R^2}H\right\} \tag{9}$$

Equation 9 describes n curves in the H-T plane corresponding to n different angular momentum states. Fig. 4 shows these curves in the H, T plane where H is in units of $\varphi_0/\pi R^2$, R is the mean radius of the cylinder and the flux quantum $\varphi_0 = h/2e$. It is assumed that the actual phase boundary corresponds to the value of the integer n, which maximizes the critical temperature $T_c(H)$. Thus the normal state is to the right of the curve for the angular momentum state giving the highest value of $T_c(H)$ for a given applied magnetic field. The general features of the curve described by Eq. 10 are reasonably transparent. The first term in the parentheses gives a periodic cusp-like oscillation of $T_c(H)$ and the second term gives a monotonic decrease of $T_c(H)$ proportional to H^2. The latter term is the same as that caused by the screening effects if the cylinder had a break in it and was singly connected. The first term results of the constraint that the angular momentum must be quantized in a doubly-connected superconductor. We find that

Fig. 4 Phase boundary between normal and superconducting states as a function of magnetic flux, $\Phi = \pi R^2 H$, and temperature.

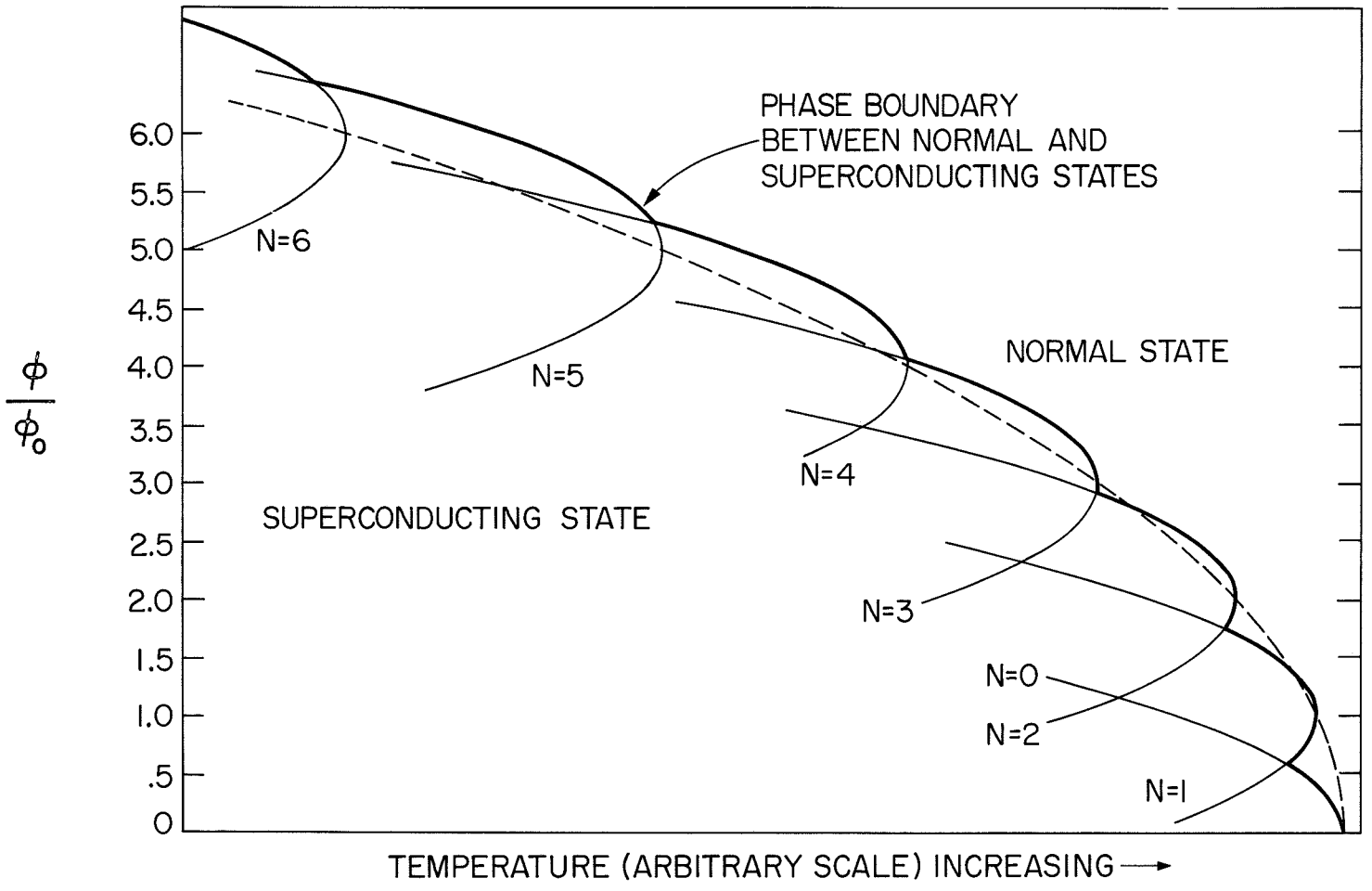

the local maxima in $T_c(H)$ to be at

$$H_{max} = \frac{n\Phi_0}{\pi R^2} \left[1 - \frac{1}{3}\frac{d^2}{R^2} + O\left(\frac{d^4}{R^4}\right)\right] \tag{10}$$

and that the difference between local maxima is completely dependent on H. A parabola passing through these local maxima in the transition temperature is

$$(\Delta T_c)_b = [\, d^2/24\,\lambda^2(o) \cdot H_{cb}^2(0)\,]\, H^2 \tag{11}$$

This background curve, is just what we would observe for a singly-connected film in which there would be no flux quantization effects.

For n = 0, we also have a parabola given by

$$(\Delta t_c)_{n=0} [\, R^2/8\lambda^2(0) \cdot H_{cb}^2(0)]\, H^2 \cdot [\, 1 + 7d^2/12R^2 + O(d^4/R^4)\,]. \tag{12}$$

The ratio of the quadratic coefficients of these two parabolas, that is, the one corresponding to the individual flux quanta at n = 0 and to the background curve is

$$\frac{(\Delta T_c)_{n=0}}{(\Delta T_c)_b} = 3\,R^2/d^2. \tag{13}$$

Preparation of samples. -- The samples were prepared by evaporating high purity aluminum or high purity indium onto rotating quartz fibers in the high vacuum evaporation system. The special substrate used to support the fiber is shown in Fig. 5. The slot in the quartz slide, across which the fiber is stretched is about 0.5 mm wide. And the substrate is bevelled below the fiber so that during evaporation there will be no shadowing. Contacts were made using silver paint.

Measurement technique. -- The special substrates carrying the complete fibers were mounted on the substrate holder shown in Fig. 6. This holder was

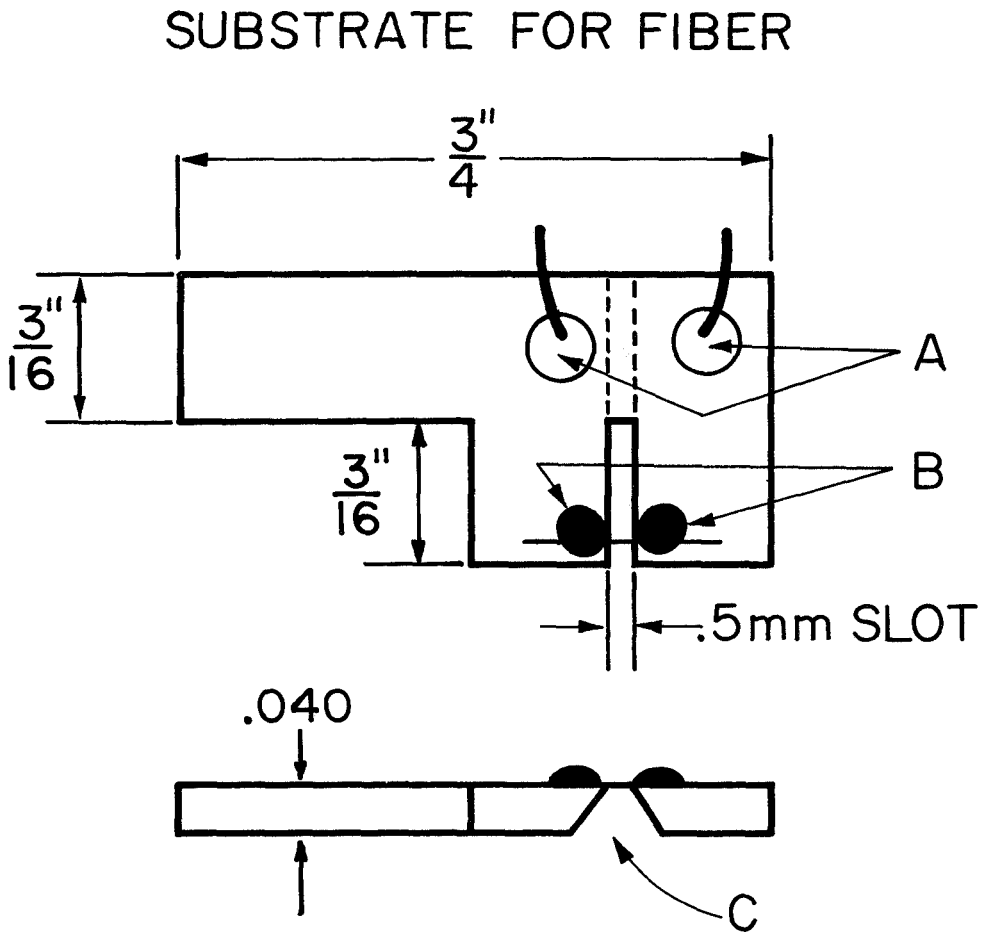

Fig. 5 Substrate for quartz fibers.

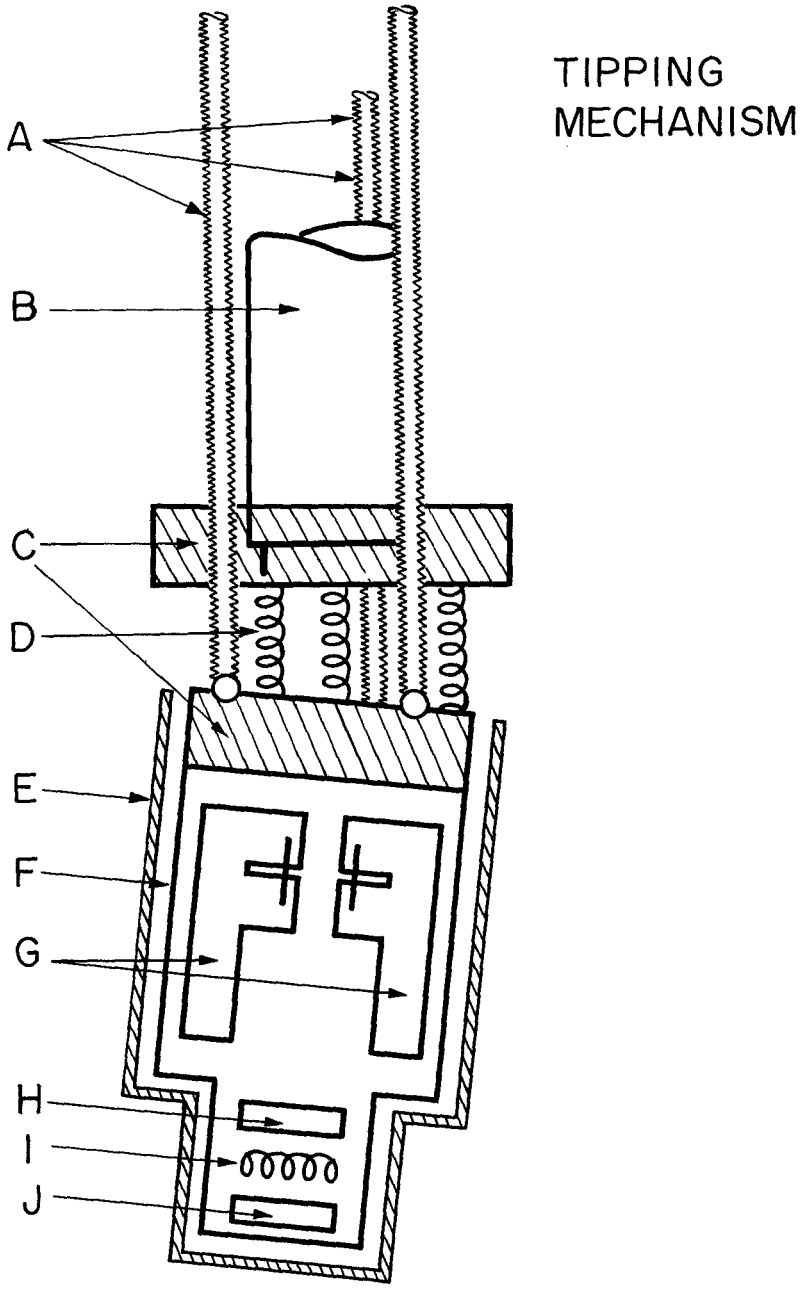

Fig. 6 Substrate holder showing tipping mechanism.

constructed so that the axis of the fiber could be tipped through several degrees about two perpendicular axes by rotating two stainless steel control rods which passed through the vacuum seals at the top of the cryostat. The angle of the fiber could be changed reproducibly by an angle as small as 3×10^{-4} radian. Two carbon resistance thermometers of nominal 10 and 50 ohm values and a 200 ohm non-inductively wound Nichrome wire heater were mounted on the holder to measure and control the temperature. The substrate holder was contained in a copper can to provide electrostatic shielding. Twisted copper leads from the samples pass through stainless steel tubes to the top of the cryostat to provide shielded voltage and current leads for the samples and separately shielded leads for the heater and thermometers.

A substrate holder was supported near the bottom of a glass helium dewar with the samples immersed in the liquid helium. On the outside of the helium dewar was fitted a copper solenoid which provided the magnetic field. The solenoid was immersed in the liquid nitrogen. The dewar assembly was surrounded by a 1/16 inch thick cylinder of Moly-permalloy to provide magnetic shielding.

The temperature of the liquid helium was measured by a 33 cycle resistance bridge and near 1°K one could control the temperature within a few microdegrees. The resistance thermometers were calibrated during each run against an oil manometer in the helium II region and against a Wallace and Teirnan dial pressure gauge at higher temperatures. A pressure measuring instrument using a bellows and a capacitance sensor (MKS Barytron gauge) was used to give the voltage proportional to the pressure of the helium vapor and thus allow recorder plots against this variable which could be readily converted to temperature.

The current source for the sample was a mercury battery with a series resistor which gave currents up to 10 micro-amperes. The voltage was measured with a battery operated dc voltmeter (Keithley 147). Voltage and current leads were individually shielded and the measuring circuit was completely isolated from the ac line except for the recorder whose power was obtained through an isolation transformer.

After mounting the samples, their resistance was measured at room temperature, and liquid nitrogen temperature, and after filling with liquid helium, at 4.2°K. As the temperature of the liquid helium was lowered below 4.2°K, the resistance as a function of pressure was plotted on the recorder using the Barytron gauge to provide a voltage proportional to the pressure. The pressure was lowered until the sample passed through the superconducting transition and showed no more resistance. A measuring current of 1 micro-amp was standardly used and it was checked if by increasing or decreasing this current by a factor of 3 changed the shape of the curve. Fig. 7 shows a typical plot near the steepest part of the resistance transition. Here the abscissa has been converted from pressure to temperature with the absolute value of the temperature determined from the calibrated resistance thermometer. After the position of the transition was located, the temperature was adjusted to be in the steepest part of the transition. The magnetic field was then raised, and the temperature lowered in such a way that the sample stayed near the steepest part of its transition, where it had about 1/2 of its normal resistance, $R_N/2$. The sample was then aligned using the angular adjustment mechanism successively tipping the cylinder to lower the measured resistance and then raising the field to again increase it. The final adjustment of angle which was made in a comparatively large magnetic field was made to within about 10^{-4} radian on each of the two orthogonal axes.

Once the cylinder was aligned with the magnetic field, the phase boundary was mapped out by holding the temperature with the regulator to $\pm 10^{-5}$ °K and then sweeping the magnetic field to plot out the resistance of the sample as a function of field at this temperature. This procedure was then repeated at a whole series of temperatures so that the complete locus of points in the H,T plane giving a certain fraction of the normal resistance was plotted out. Such data is shown in Fig. 8 and from a large number of such curves the phase boundary in the H,T plane could be constructed. To do this the assumption was made that the position of the phase boundary is the point at which the resistance of the sample is one half of the normal resistance. The validity of this assumption will be discussed later.

Fig. 7 Resistance transition curve. Resistance of microcylinder versus temperature.

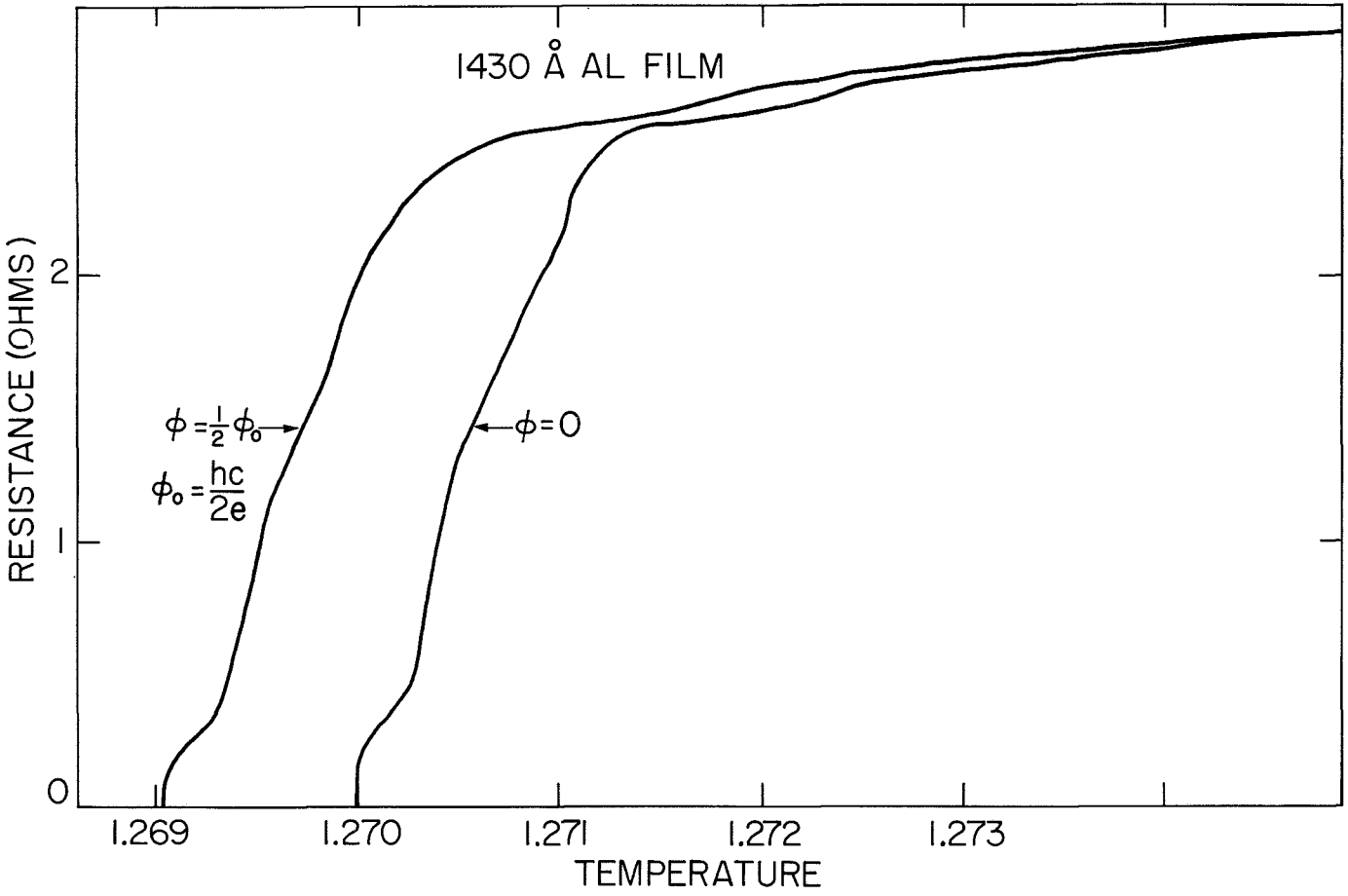

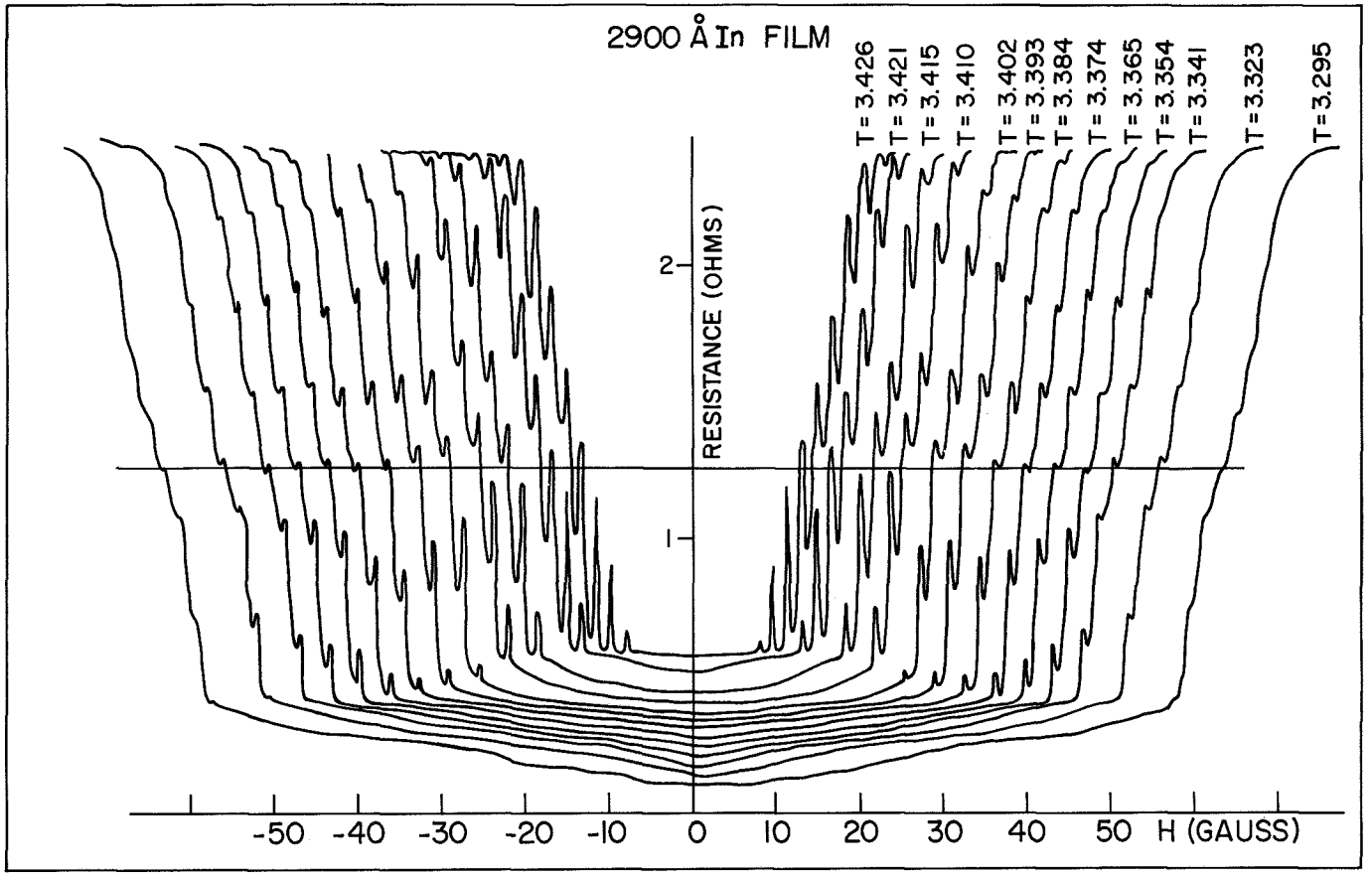

Fig. 8 Data showing resistance as a function of field for various temperatures for a 2900 Å indium film.

The dimensions of the film were measured optically. The length (approx. 1 mm) was determined by a measuring microscope. The diameter was measured approximately by means of a micrometer filar eyepiece on an optical microscope, but because of the diffraction effects, this measurement was not accurate enough to use in analyzing the results. The diameter used was that calculated theoretically assuming the correctness of flux quantization. The thickness of the evaporated film was measured by the method of equal chromatic order of a multiple reflection interferometer. This measurement was actually done on the flat portion of the fused quartz substrate. Provided the accomodation coefficient of the quartz fiber and the quartz substrate are the same, the thickness of the evaporated cylinder on the fiber should equal that of the plane film on the substrate.

Measurements. -- Measurements were made of the phase boundary in the H, T plane for aluminum films in thicknesses from 340 to 2000 Å. Typical original data is shown in Fig. 8. From such data plots of the variation of transition temperature with magnetic field could be found. Fig. 9 shows the variation of transition temperature with magnetic fields near $H = 0$ in the zero angular momentum state. As predicted by Eq. 9 with $n = 0$ and $H \longrightarrow 0$ the decrease in transition temperature is quadratic in magnetic field. (See Fig. 10.) When the maxima in T_c are plotted as a function of field, the so-called background term, they are also quadratic in magnetic field, as predicted by Eq. 9. Figs. 11 - 13 give typical examples of this quadratic behavior. From curves similar to these, we can obtain the quadratic coefficient of the background term and of the term for $n = 0$. The ratio of these quadratic coefficients as measured and from the theory was found to be in close agreement over the whole range of film thickness. Similar results were obtained from a small number of indium films. The plots of the lowering of the transition temperature as a function of magnetic field for one of these films is shown in Fig. 14 for the background case.

Fig. 9 Variation of the transition temperature with magnetic field for the zero angular momentum state in a 2500 Å aluminum cylinder.

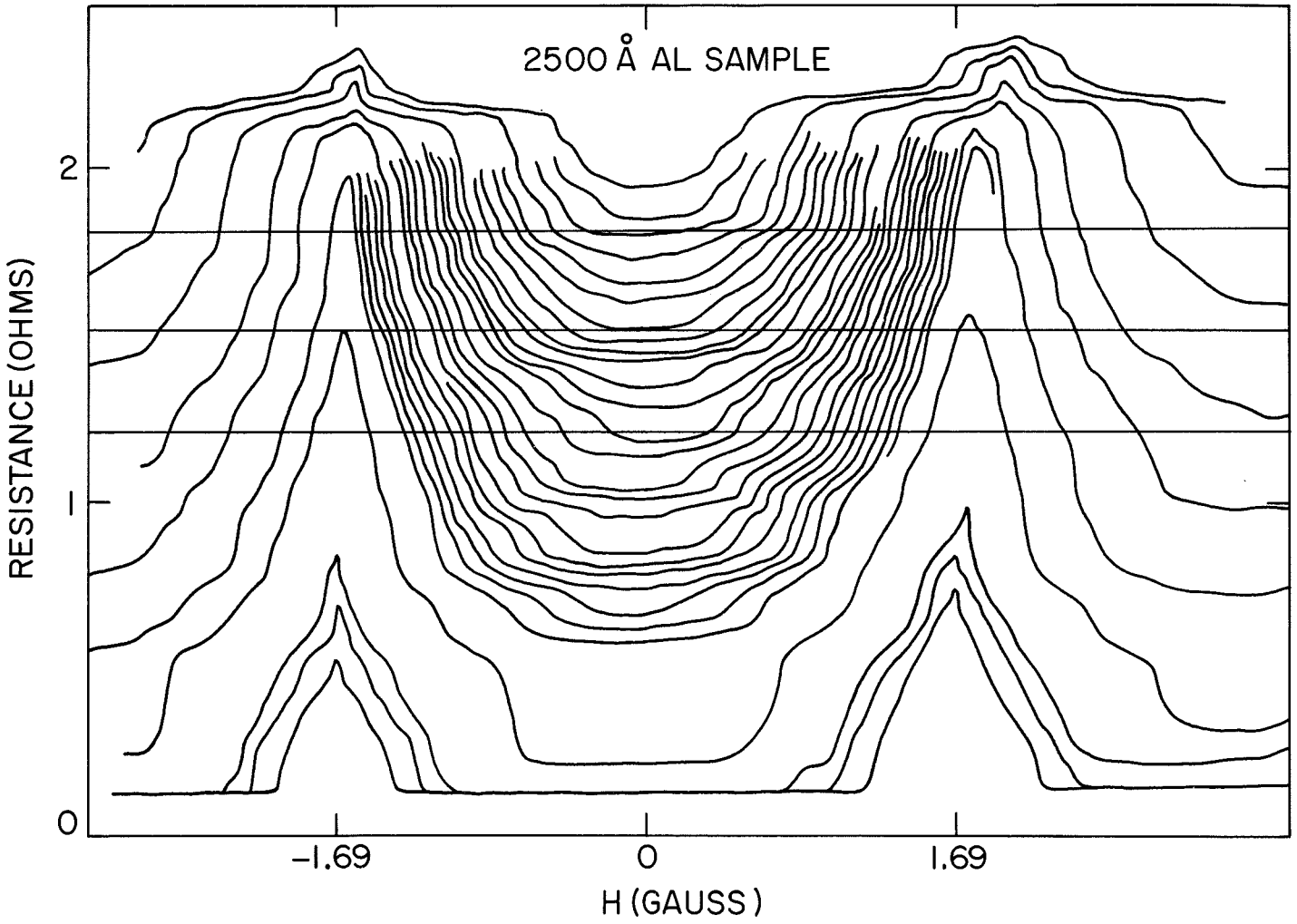

Fig. 10 Transition temperatures plotted against magnetic field for n = 0, 2500 Å aluminum.

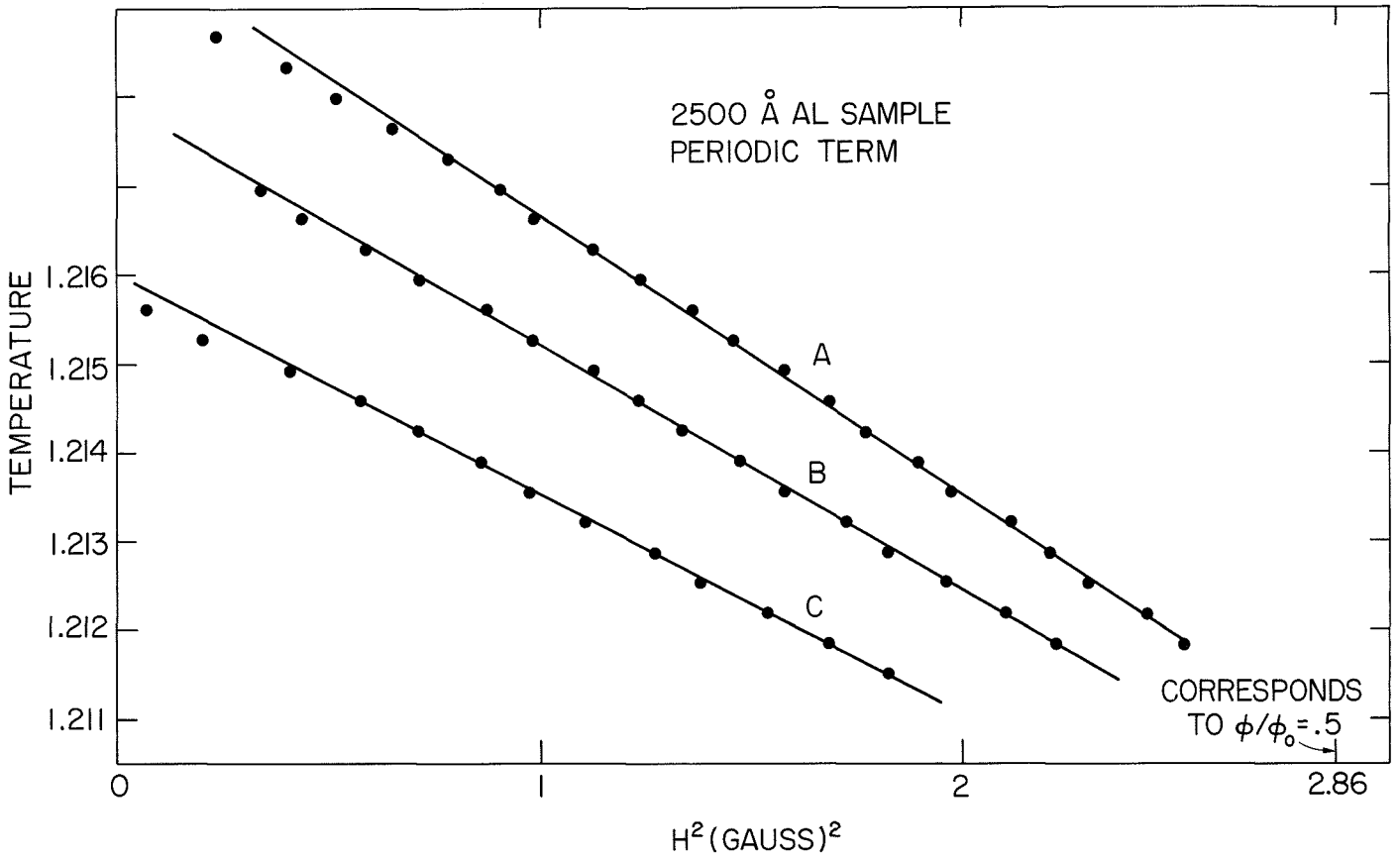

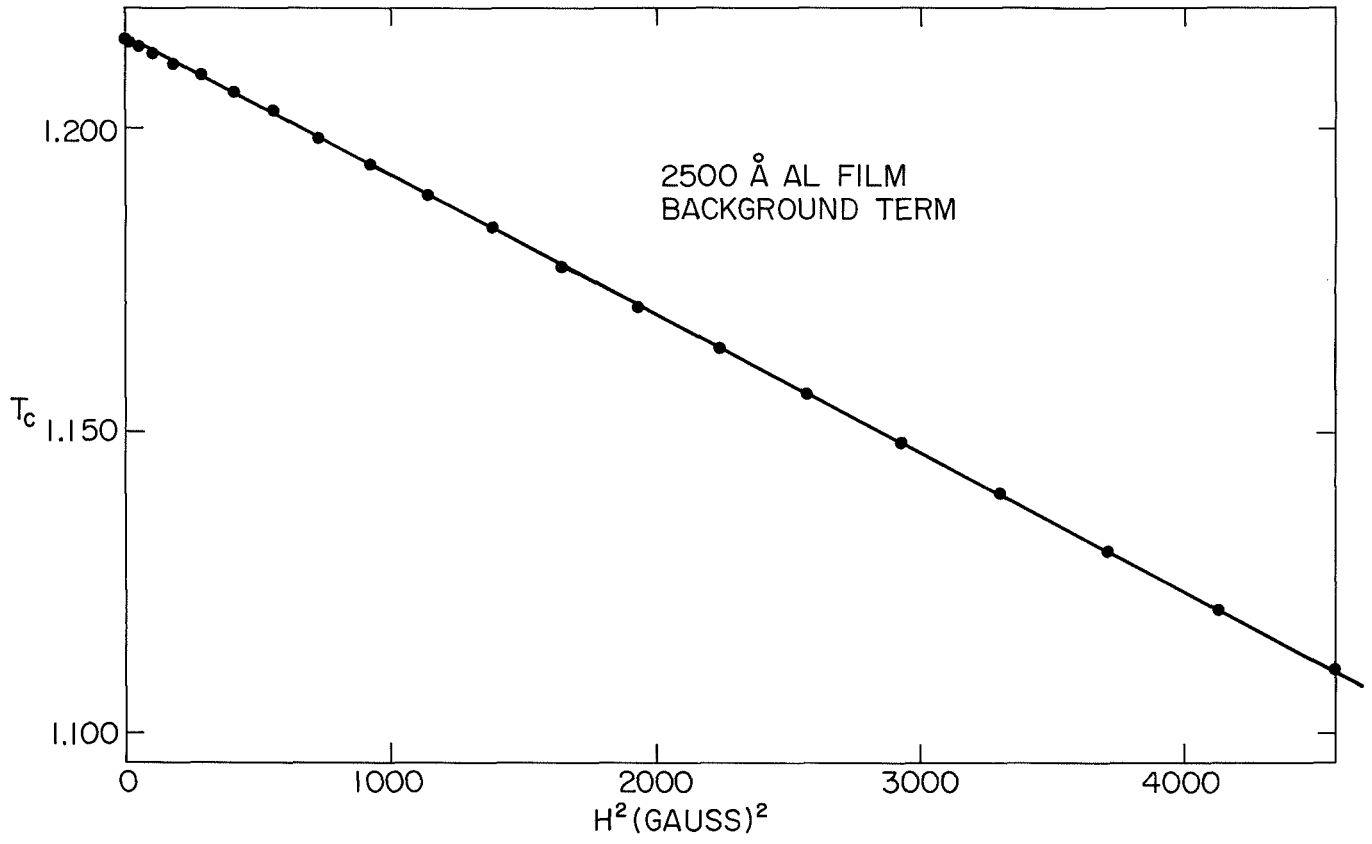

Fig. 11 $(T_c)_{max}$ versus H^2, 2500 Å aluminum.

Fig. 12 $(T_c)_{max}$ versus H^2, 340 Å aluminum.

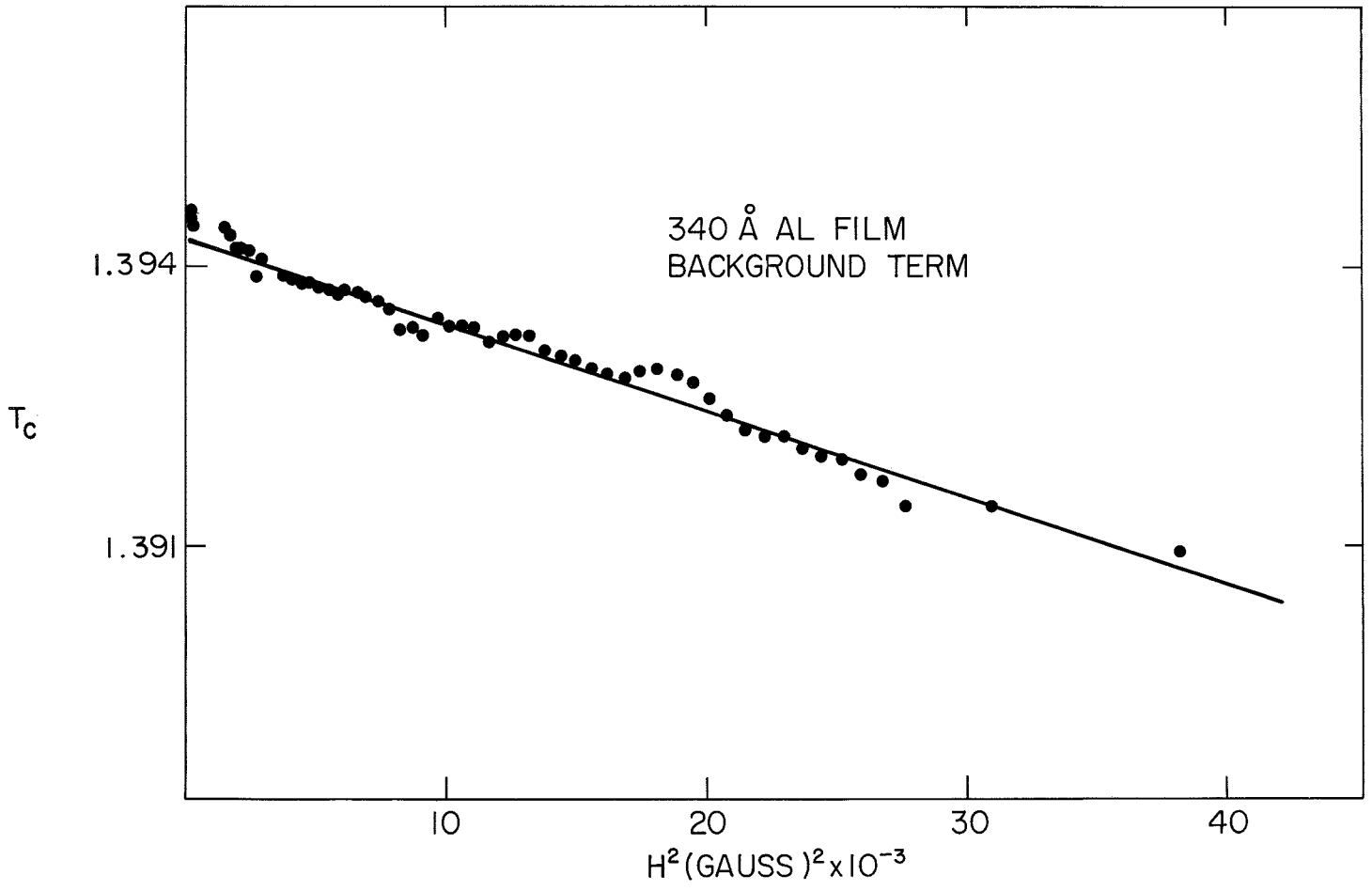

Fig. 13 $(T_c)_{max}$ versus H^2, 984 Å aluminum.

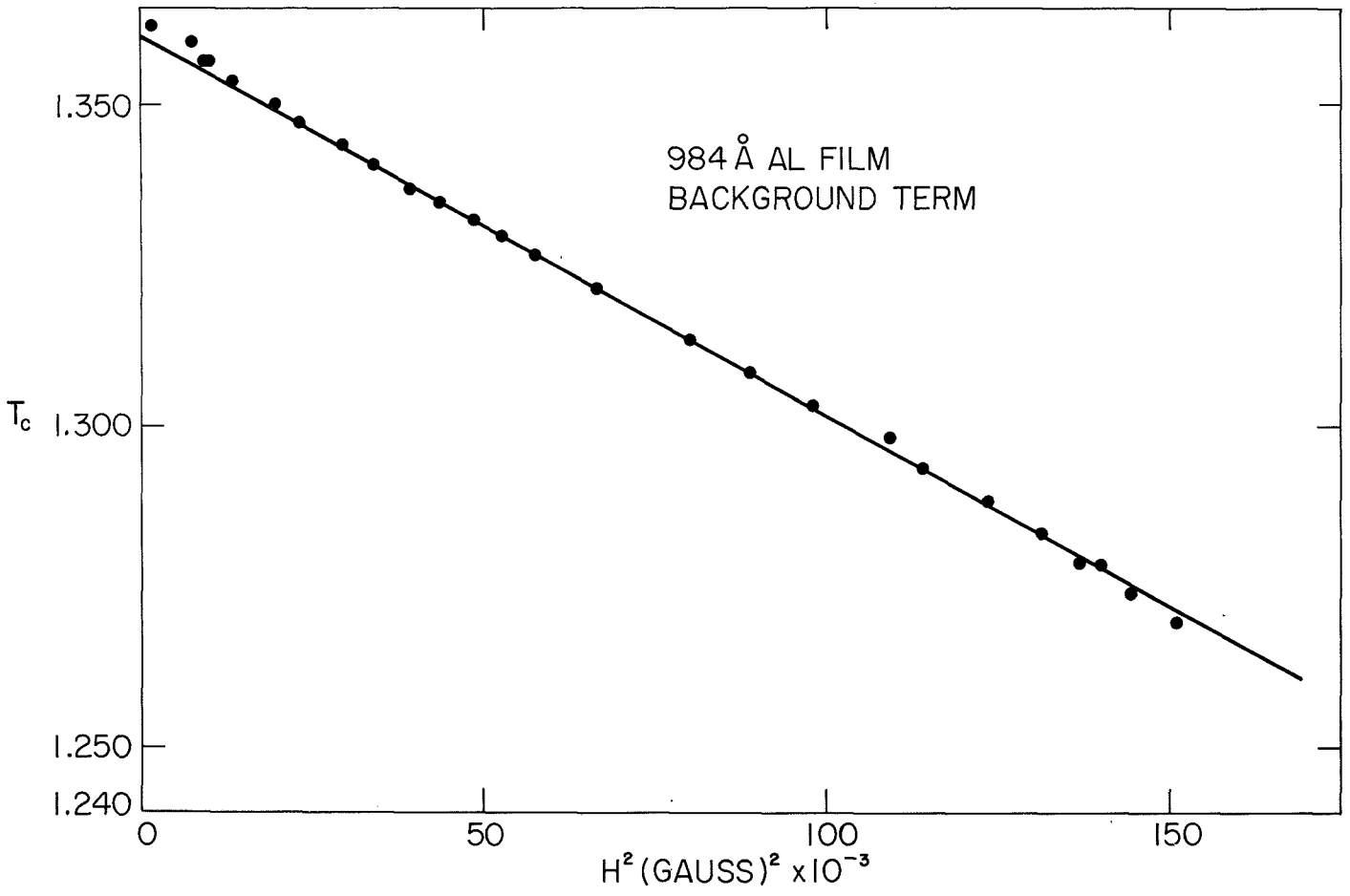

Fig. 14 $(T_c)_{max}$ versus H^2, 2900 Å indium.

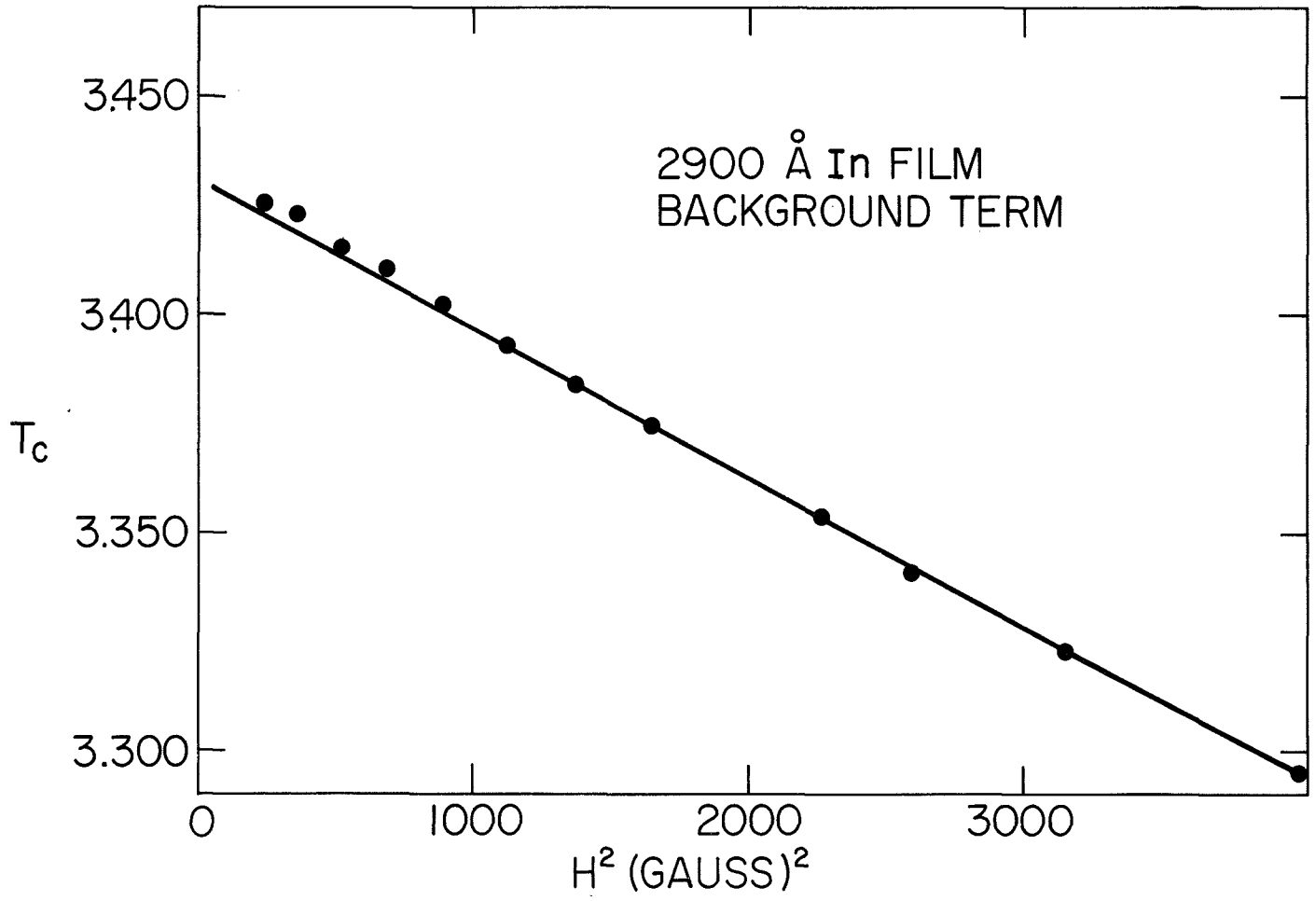

After the phase transition was mapped out in the parallel field case, $\theta = 0$, the angular dependence was measured. For very small angles this agreed well with the Tinkham theory Eq. (9) but for larger angles the deviations were significant. In addition it was found that in the low resistance region some of the flux quantization peaks split into twin peaks. Presumably this effect was caused by flux lines piercing the wall of the cylinder and forming a more complex current pattern. It was shown that the splitting of the flux quantization peaks (minima in T_c) was proportional to the perpendicular magnetic field.

Additional investigations.-- A search was made for the effects of higher order correlations, that is, the effects to be expected if the electrons not only form pairs, but were grouped in higher numbers, such as 4, 6, 8, etc. Such high order correlations would be expected to lead to additional cusp-like structures on the transition temperature versus H curve, as shown schematically by Fig. 15. A careful search for such effects was made using a method of measuring the second derivative of the resistance versus H curve. In the absence of higher correlations or other interfering effects, these curves are quadratic and therefore have a constant second derivative. Additional cusps added to such curves should show up as non-uniformities in the second derivative in particular places in the flux quantization cycle. No such effects were definitely seen, although a great deal of structure was found on the second derivative curves, and was even noticeable on the curves of resistance versus field. Such structure turned out to be mostly caused by structure in the resistance transition. In certain instances, regular steps in resistive transition were seen as shown in Fig. 16. These steps are presumably of some basic interest, but as yet no explanation has been offered.

The effect of fluctuations was apparently observed in one of the thin films. In this case, when the depression of the transition temperature was plotted as a

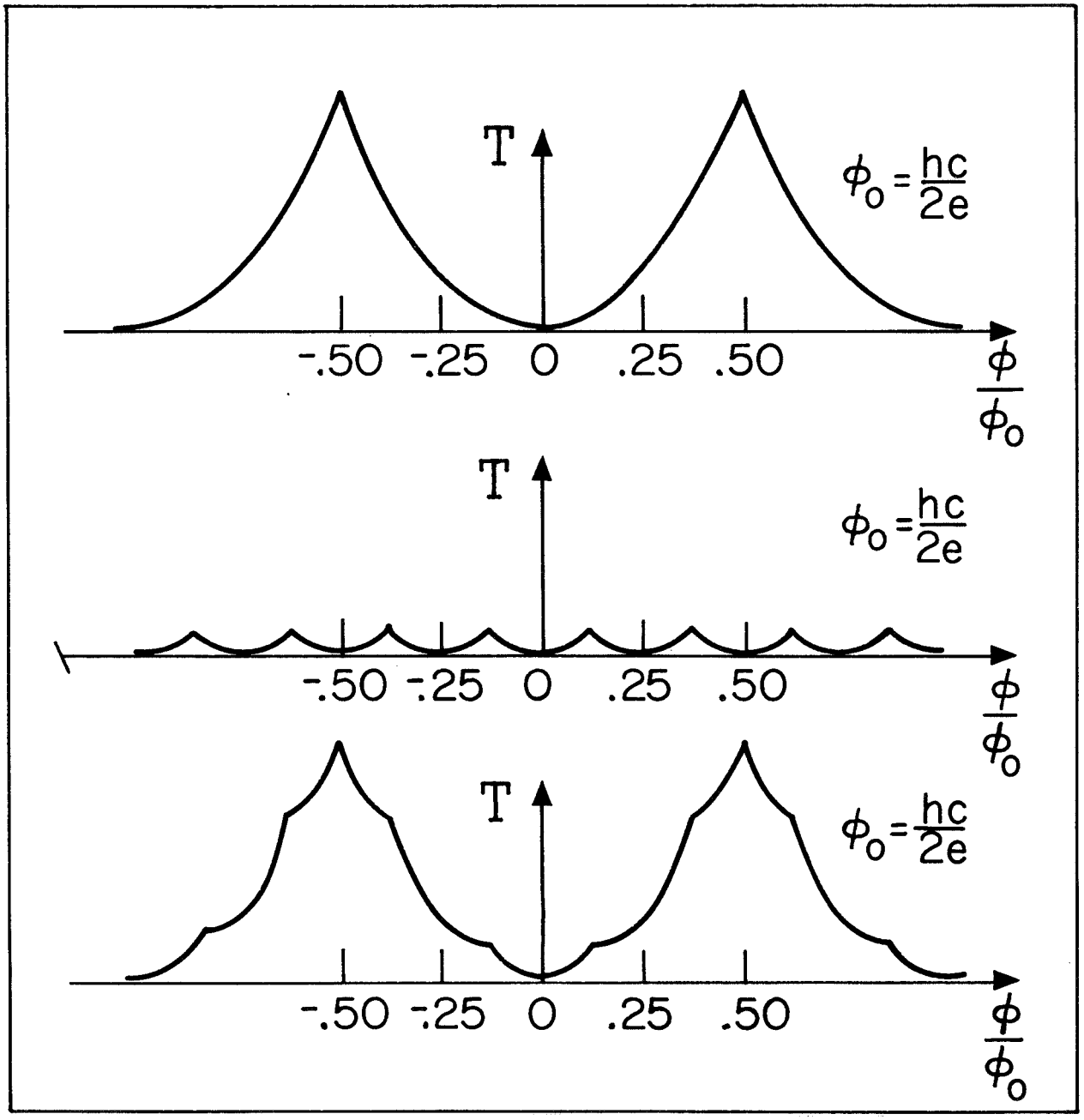

Fig. 15 Conjectured shape of phase boundary in the case of higher order correlations by quartets of electrons in addition to pairs.

Fig. 16 Measured step structure on the resistance transition of an aluminum cylinder.

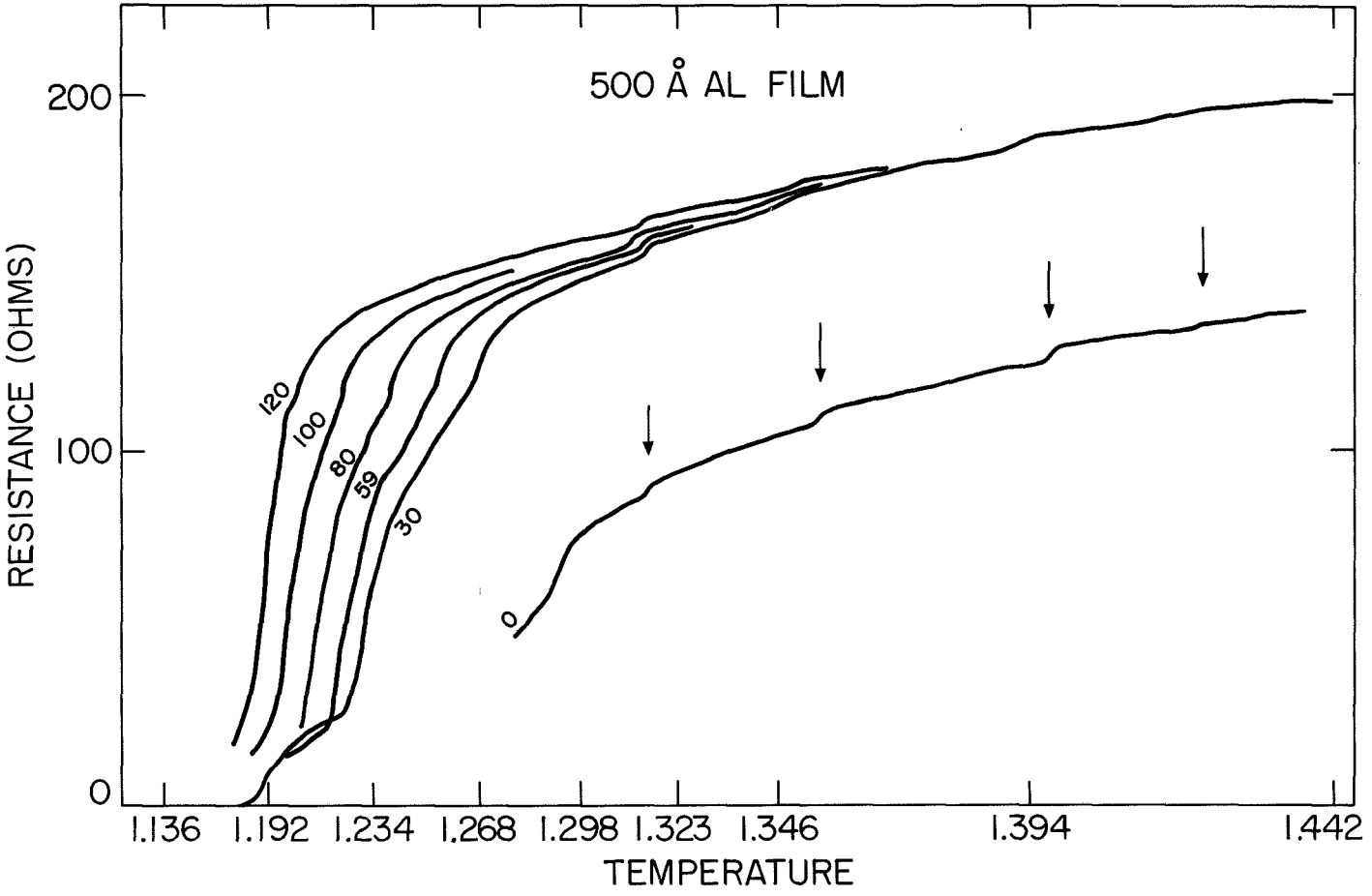

function of magnetic field squared, the result was a straight line for low values of resistance corresponding to the lower part of the transition curve but deviated from a straight line for higher values of resistance in the upper part of the transition curve. It is believed that these effects are due to fluctuations in the film above the true thermodynamic transition temperature. Plot of ΔT_c versus H^2 is shown in Fig. 17 and is perhaps what one would expect from fluctuations in the region above the true thermodynamic transition.

The effect of the measuring current on flux quantization effects was also investigated. It had been reported by Spence (Ref. 12) that the amplitude of flux quantization effects in vanadium films decreased drastically when the De Broglie wave length of the measuring current approximately equals the diameter of the cylinder. In measurements made with Al films which were 6.35 μ in diameter and 434 Å thick, no such effects were observed.

Temperature dependence of the magnetic field periodicity. -- During the course of these measurements, it was discovered that there was a temperature dependence of the magnetic field periodicity in flux quantization (See Fig. 18). Such an effect, if it were found to be a fundemental effect, could limit the accuracy of flux quantization measurements and destroy their claim to absolute accuracy based on the constant h/2e. A study of this effect was made and two possible explanations were proposed. The first assumes that the effect is caused by variations in thickness in the thin films, and is caused because the transition temperature is also a function of thickness. This leads to an effective variation of cylinder radius with temperature and thus a change in the measured periodicity. If this explanation is correct any fundemental inaccuracy can be avoided by more uniform or thin films. The second explanation, which could not be entirely excluded, is that the effect is caused by fluctuations at the transition temperature. A short summary of this result was published (Ref. 13). To differentiate between the two explanations it would be possible to measure the periodicity of much thinner films in which fluctuation effects should increase but the possible variation of effective radius would decrease.

Fig. 17 Depression of T_c as a function of magnetic field showing the deviation from quadratic dependence which may indicate the effect of fluctuations.

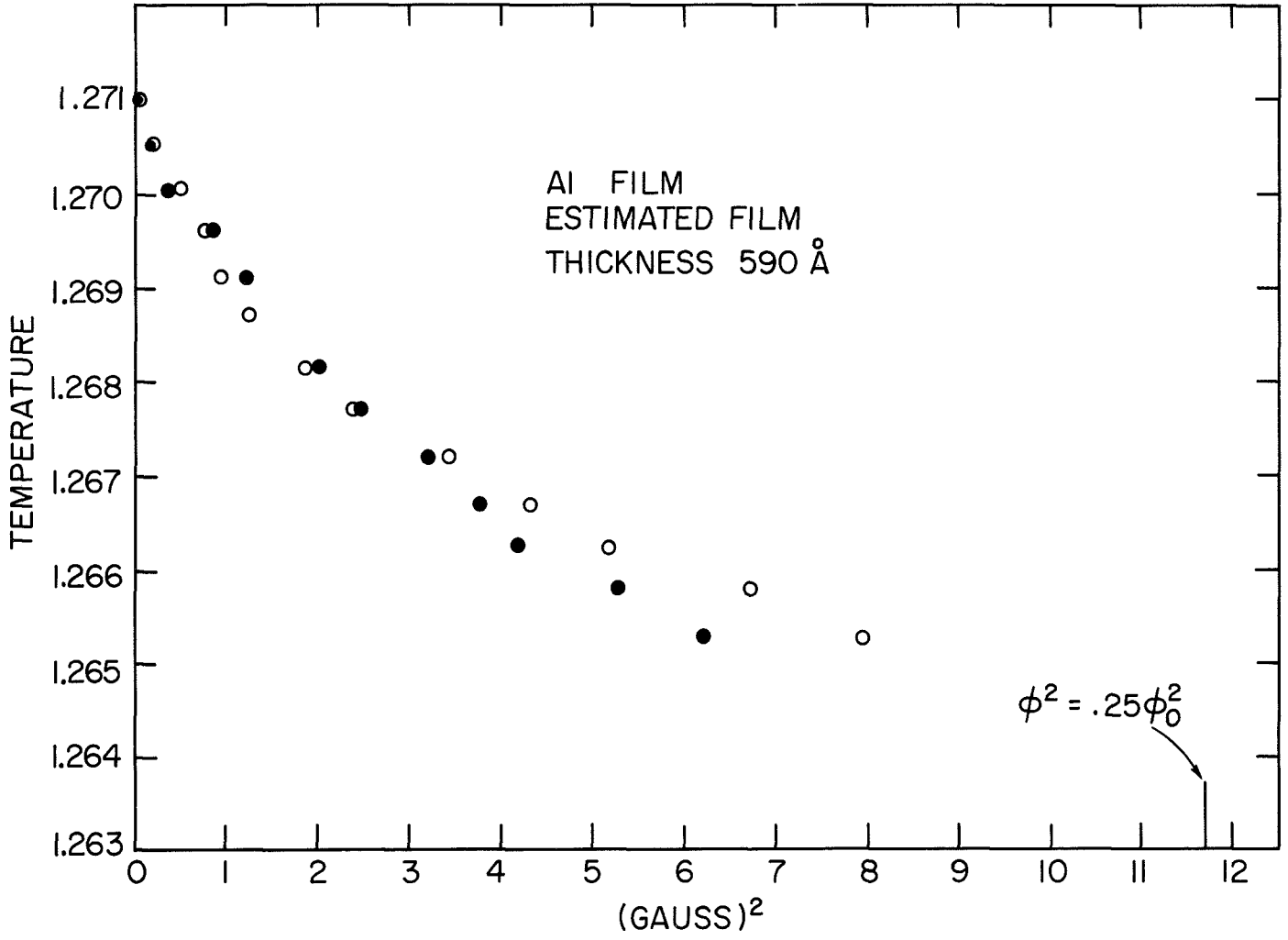

Fig. 18 Observed temperature dependence of the magnetic field period in thin aluminum cylinders.

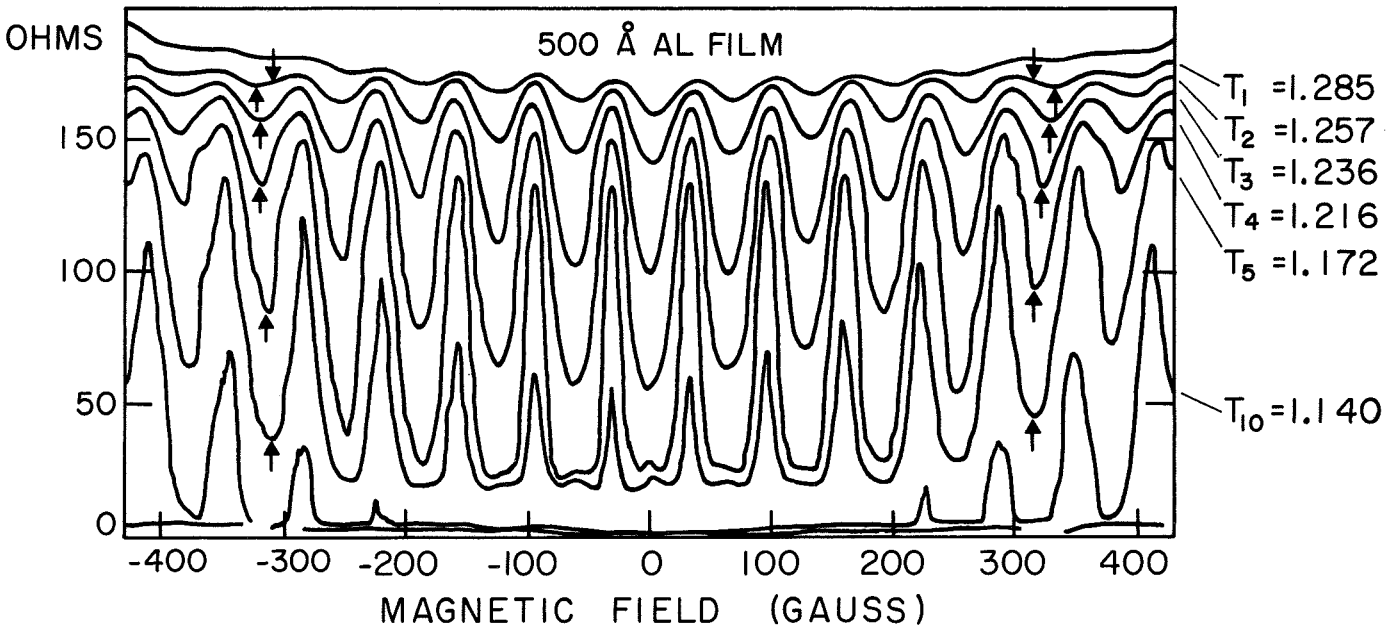

Fig. 19 Schematic digram showing model of film of how a variable thickness could give a temperature dependence of the field period.

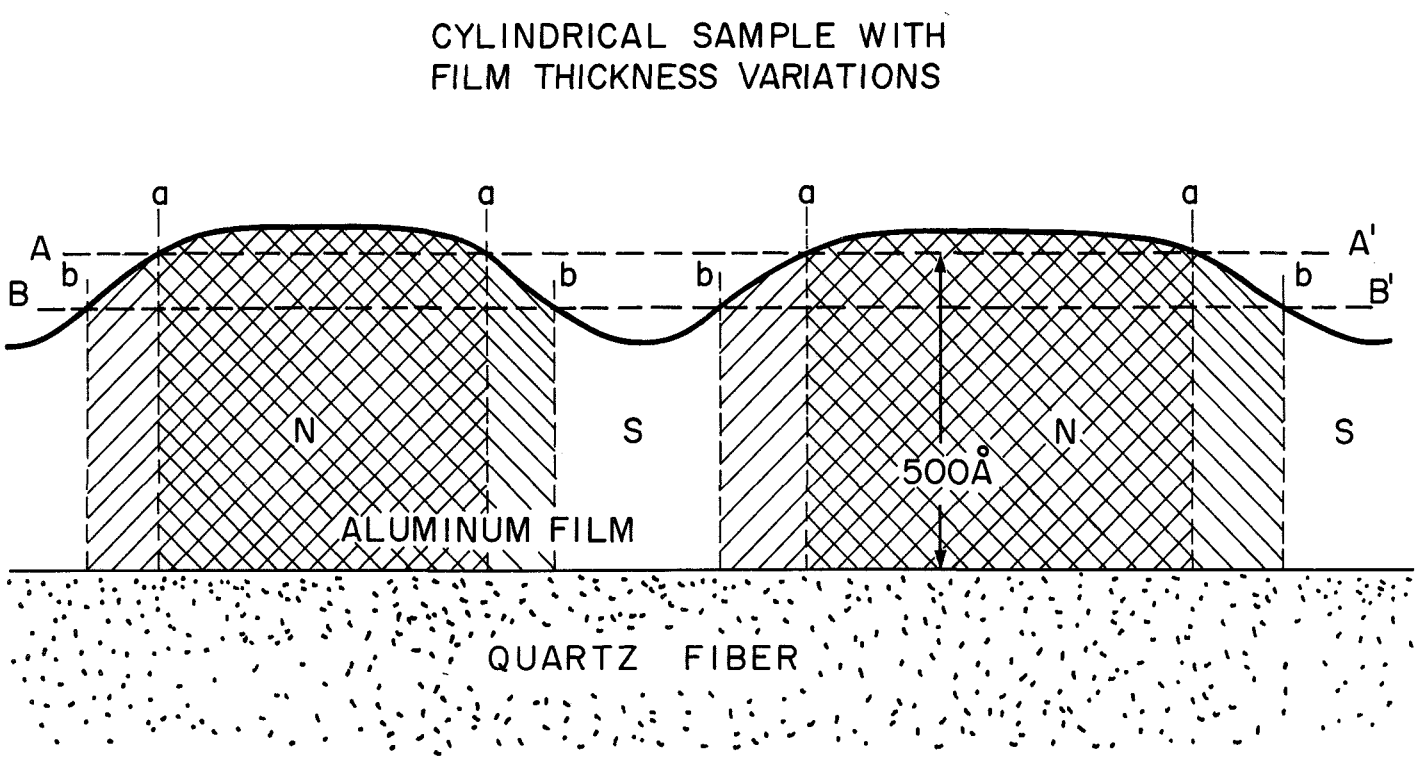

Magnetometer and Ammeter

The discovery of flux quantization made possible the development of new instruments to measure flux in a digital way in units of $\frac{h}{2e} = 2.068 \times 10^{-7}$ gauss cm^2. Since this is a small amount of magnetic flux, such digital measurements, in units of the fundemental constant $\frac{h}{2e}$, offer great advantages in precision. They are analogous to the highly precise measurements of frequency and time and the measurements of length by interferometry. In addition to simply measuring the flux, it was realized that this method could be used for measuring all the electromagnetic quantities because the magnetic flux is dimensionally equal to the product of magnetic induction and area or current and length or voltage and time.

$$\varphi = B L^2 = \mu_o I L = Vt \qquad (14)$$

The significance of this is that length and time are quantities which can be measured with more precision than most. Now if we include magnetic flux in this category, the measurement of current and voltage can in principle be measured with similar precision. Since most scientific measurements are made by electrical methods the potential improvement in accuracy and ease of precision electrical measurements should be significant. One of the major goals was to investigate the feasibility of such instruments. For this purpose, a magnetometer and an ammeter were built.

Magnetometer. -- The essential part of the magnetometer was a split ring machined from high-purity niobium (Ref. 14). The interior diameter of the split ring was approximately 2 mm. The two halves of the ring were separated by Mylar sheets 12 microns thick. Two niobium screws (No. 000-120) were threaded through one half of the split ring and their pointed ends pierced the Mylar sheet and formed two superconducting contact points on the other side of the split ring. The plane of the ring was horizontal so that a sample could be inserted from the top of the dewar system and inserted in the magnetometer ring without having to raise the magnetometer to room temperature. The niobium screws could be adjusted from the top of the dewar by means of two control rods and a worm gear arrangement

which gave slow motion at right angles to the control rods. The control rods were made so that they could be disengaged after adjustment. This was to eliminate this source of vibration on the superconducting contacts.

To eliminate magnetic background the magnetometer housing was made of very high purity copper. The three support rods of the magnetometer housing were made of phenolic plastic which was both non-magnetic and a thermal insulator. The magnetometer assembly was housed in a glass dewar system. Auxiliary electrical leads were provided for two carbon resistance thermometers and a resistance wire heater. This allowed the temperature to be measured and controlled electronically. Fig. 20 shows the magnetometer assembly. Fig. 21 shows a close-up view of the gear box and niobium ring assembly.

The magnetometer was built and put into operation. In the initial trials the superconducting contacts were biased by a current of about 10^{-4} amperes and the voltage across the contacts was measured by a dc voltmeter. The magnetic field periodicity was approximately 10^{-5} as expected and the periodic voltage was of the order of 10^{-7} volts. Because of ambient magnetic noise it was necessary to use a superconducting shield. Using a lock-in detector at 500 cycles it was possible to detect a change of approximately 10^{-8} gauss.

The magnetometer was used chiefly as a prototype to investigate the capabilities, limitations, and the critical design features of such an instrument. While the instrument was very sensitive when in operation, its operation was intermittent for a number of reasons. To begin with,the mechanical system used to adjust the niobium points was not satisfactory. The long control rods, which extended from the low temperature region to the top of the dewar coupled to the worm gear system led to the large amount of backlash. It proved to be a tedious job adjusting the niobium points which were extremely sensitive. Some of this difficulty was avoided by installing stiffer control rods and tightening up the gear system, but it appeared that the basic difficulty remained. The system of advancing a screw never could be made to form a reproducible contact. This is hardly surprising when we consider the crudeness of the macroscopic adjustment and the fact that the critical area of

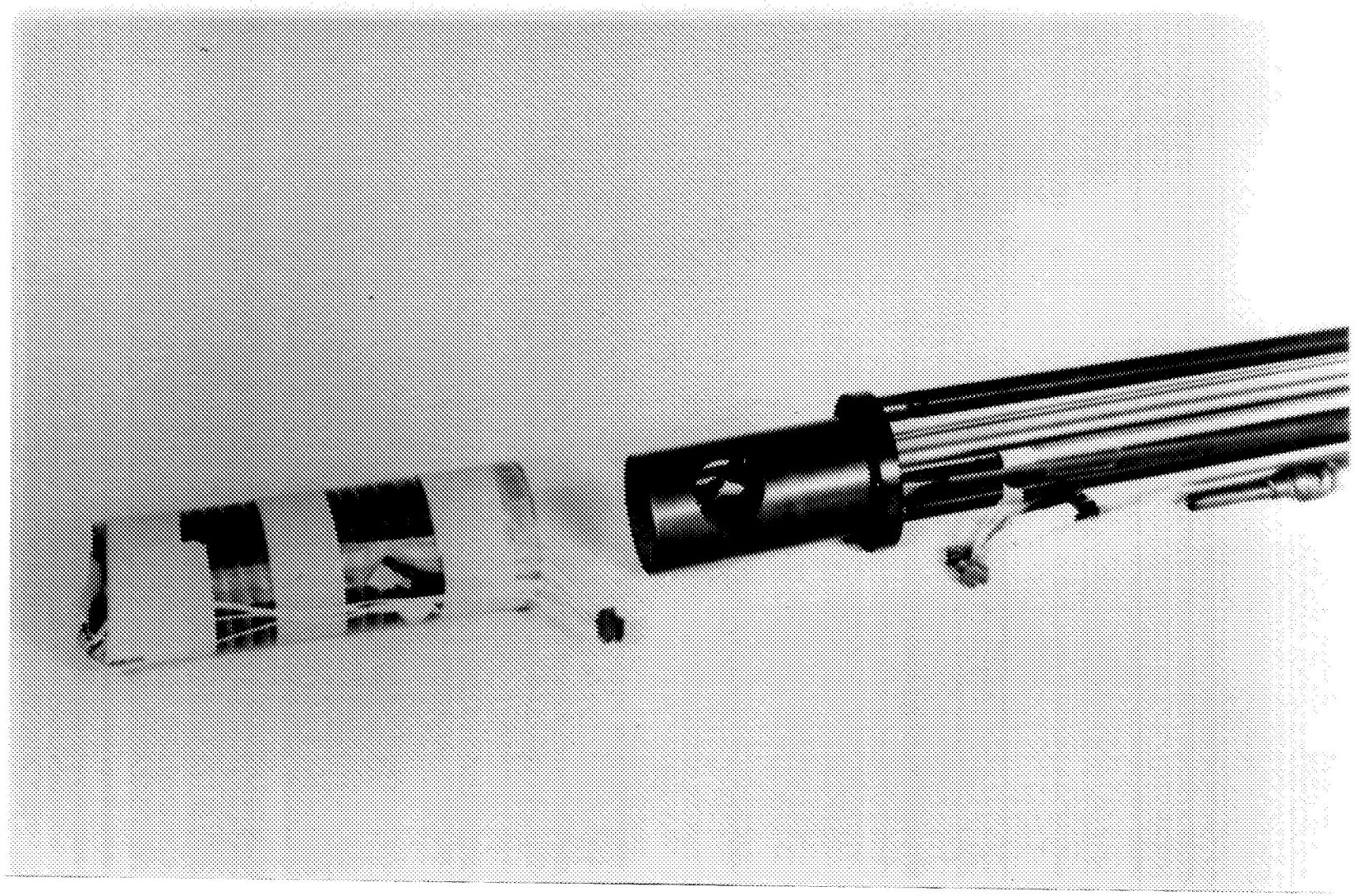

Fig. 20 Magnetometer-ammeter prototype, with solenoid in place.

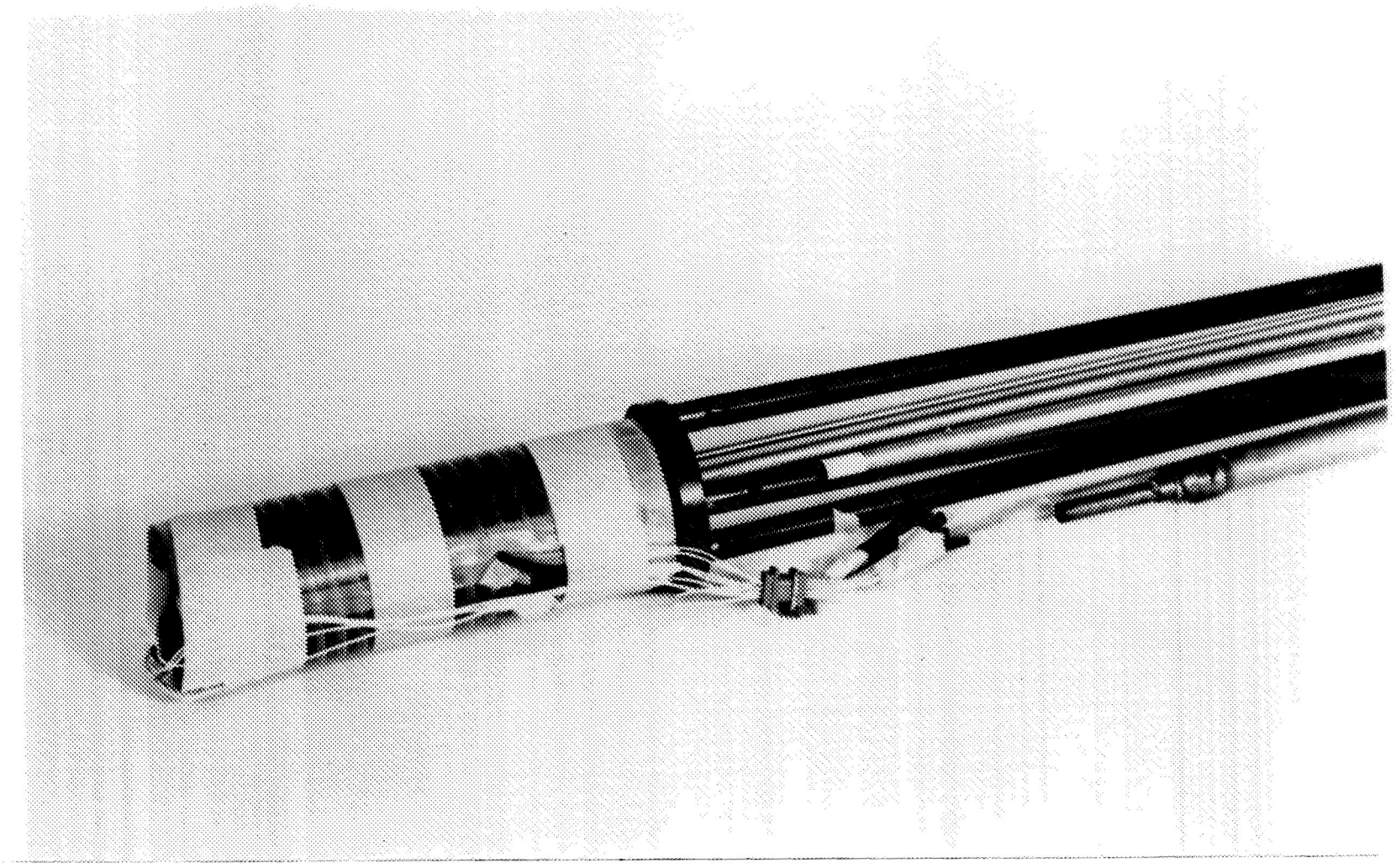

Fig. 21 Magnetometer-ammeter prototype, solenoid removed.

contact is probably less than a micron square. It was always possible to obtain contacts which could operate but the voltage signal from these contacts as a function of magnetic field was not simply periodic with the field but had a great deal of additional structure, probably due to the fact that there were a number of contacts rather than a single contact. It was this complex structure which was not reproducible from one setting of the contacts to the next and which could not survive heating to room temperature and would often change for no obvious reason, probably due to external vibrations or to an electrical transient to the measuring current. The complex nature of the voltage signal as a function of field made a reliable system for counting fluxons over a large change in field very difficult and probably not practical to use in a reliable instrument.

It was concluded, therefore, that the bulk niobium split ring with a screw contact was a poor basic element around which to build a reliable magnetometer. The effort therefore changed to developing thin film rings with point contacts which might prove to be more reliable and stable.

Ammeter and measurement of the flux quantum. -- The magnetometer was originally designed to be converted into an ammeter. For this purpose a copper mount was provided for a quartz cylinder, on which was evaporated a thin film superconducting ring (See Fig. 22). This superconducting cylindrical ring was coaxial with, and exactly in the center of, a precision solenoid. The solenoid was made on a very pure copper form and was wound with a single layer of formvar insulated No. 30 copper sire. The copper cylindrical form was very precisely machined and a shallow helical groove was turned to hold the copper wire in exactly even spaced and known positions. The superconducting thin film cylinder was evaporated on a precision ground and polished quartz cylinder whose diameter could be measured to within approximately 1 micro-inch using a fringe counting micrometer. The instrument was tried with a 400 Å thick aluminum film which was scribed longitudinally so that two large area regions of the thin film were connected by a constricted thin film bridge about 10 microns wide on opposite sides of the rod. The detection circuit is shown schematically in Fig. 23.

Fig. 22 Sketch of proposed ammeter showing the inner fluxon detection loop and the outer thin film solenoid.

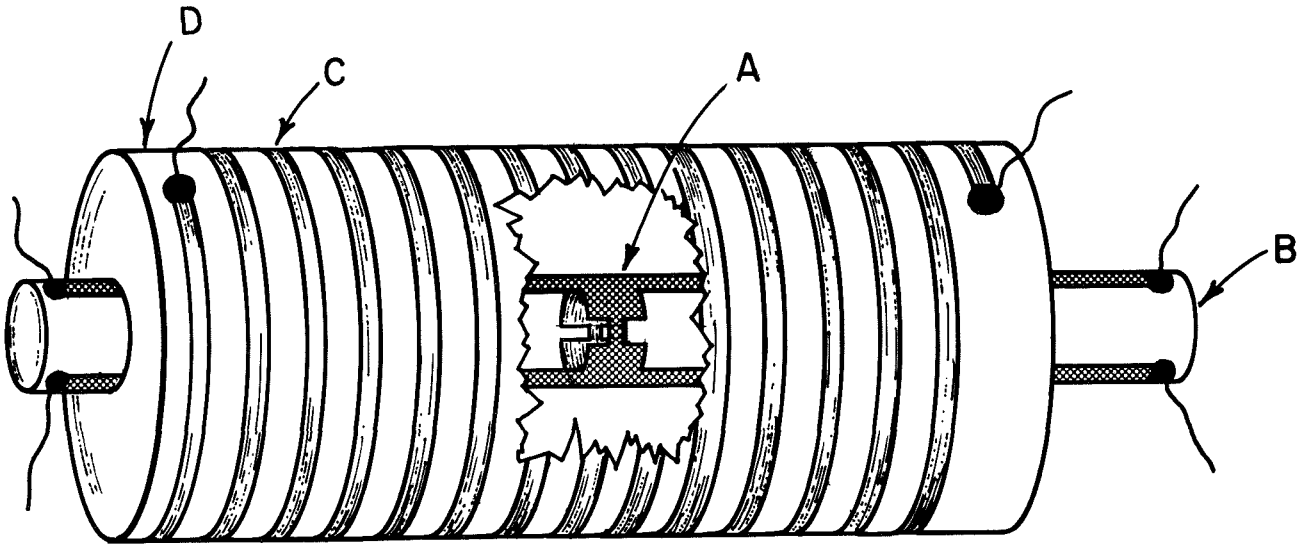

Fig. 23 Schematic of the circuit for the detection of flux quanta.

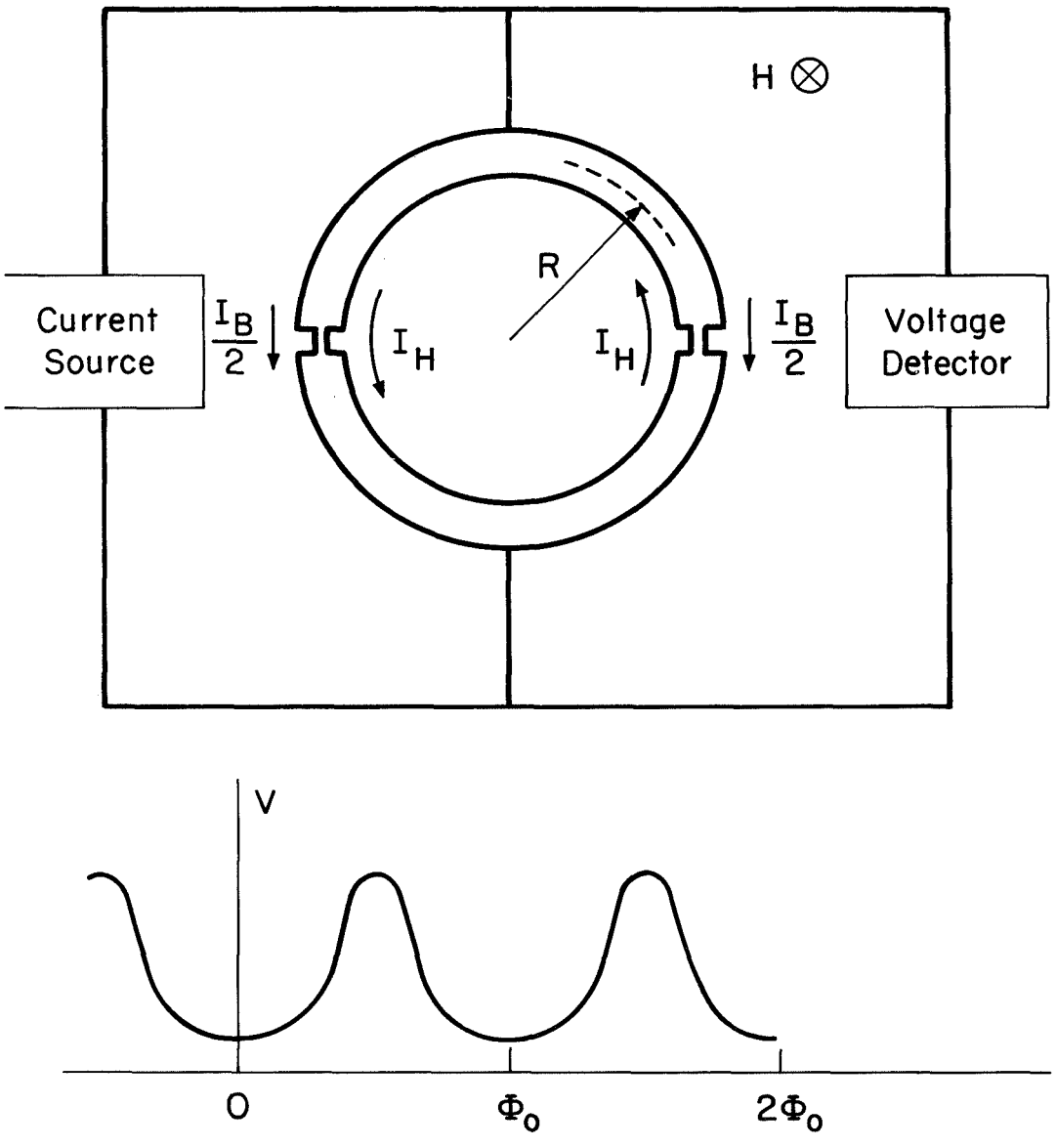

A voltage periodic with field was obtained from the thin film ring with approximately the expected periodicity. These thin film rings had various drawbacks. They were quite sensitive to perpendicular fields and to the alignment of the cylinder. They contained, aside from the periodicity, many other variations of the voltage vs. field. These features were not always reproducible and indeed tended to change discontinuously because of transient current pulses induced from outside electrical sources. Because of the ambient magnetic noise it was found to be essential to operate with a superconducting shield in place. On the basis of these preliminary experiments and on a theoretical study of the second order effects due to the finite thickness of superconducting film the design of a precision ammeter was proposed (Ref. 15). In this proposal it was concluded that an instrument of this type could make a precision current measurement in terms of the flux quantum, a measurement which would be limited in accuracy by the determination of the cross sectional area of the quartz cylinder. It was concluded that this area could be determined to one part in 10^5 without enormous effort and that by a very great effort it could be determined to perhaps one part in 10^6. Another method of using the thin film ring was also suggested which avoided the basic difficulty of measuring the very small cross-sectional area of the cylinder to very great accuracy. This method could perhaps give a measurement of the ampere in terms of the flux quantum and the standard ohm to greater precision than one part in 10^6.

It had originally been planned to make a fairly high precision measurement of the flux quantum using the thin film ring and precision solenoid. However, because of the necessity for a superconducting shield it would have been necessary to redesign the dewar system to take a very much larger and more precise superconducting shield which would have perturbed the solenoid much less and to a calculable degree. In the meantime, however, the voltage frequency relation implied by the ac Josephson effect had been measured by Parker, Taylor, and Langenberg (Ref. 16). Although their measurement of $\frac{h}{2e}$ is not precisely the same as the measurement of the flux quantum, there is very good reason to believe theoretically that if the Josephson frequency-voltage relationship is exactly valid then the flux quantization relation is also exactly valid. The Josephson relation has now been

shown to hold approximately one part in 10^6 so that it was not considered necessary to make the less precise measurement using flux quantization since the scientific basis for believing that the flux quantum is exactly $\frac{h}{2e}$ seemed completely established. It was concluded that the main improvement needed to make magnetometers and ammeters of very high precision and reliability lay mainly in the fabrication of the thin film constrictions and junctions and in the methods of detecting the field perdiocity exhibited by such junctions when in a thin-film ring.

Kinetic Inductance

From the investigations described above it was concluded that the basic problem of developing flux quantization instruments lay in the production of weak superconducting links having the proper characteristics. Such links seem to be essential in all the methods used for the detection of flux quantization effects. Whether these were Josephson junctions, niobium point contacts or thin film bridges the principle on which detection of flux quanta was based is essentially the same. The external magnetic field acting on a superconducting ring induced a circulating current. This circulating current passing through the link increased kinetic energy could then be detected by a decrease in transition temperature or an increase in the resistance of this localized area. Thus the basic problem of detecting fluxons led directly to the study of how the kinetic energy of such regions depended on the current. Put in other words, the essential property of these thin film superconducting links was their nonlinear kinetic inductance.

Concept of kinetic inductance. -- Kinetic inductance is essentially the inertial mass of the current carriers and the concept arises naturally from the expression for the energy associated with an electric current carried by particles of mass m and number density n.

$$E = \int_{\text{all space}} \frac{1}{2}\mu H^2 \, dr + \int_{\text{conductor}} \frac{1}{2} m v^2 \cdot n \cdot dr. \qquad (15)$$

For a homogeneous conductor of uniform cross section and uniform current density

whose material properties such as μ, n, m, e are independent of H and J we can write Eq. (1) as

$$E = \frac{1}{2} L_M I^2 + \frac{1}{2}[(m/ne^2)\cdot(l/\sigma)]I^2 . \tag{16}$$

Here the first term is the magnetic energy and L_M is the usual magnetic inductance. The kinetic inductance is the quantity in parentheses in the second term.

$$L_k = (m/ne^2)\cdot(l/\sigma). \tag{17}$$

The material of the conductor enters by the factor $\Lambda = m/ne^2$ and the geometry by the factor l/σ, the length divided by the cross-section area.

The concept of kinetic inductance is inherent in the London theory of superconductivity in which the energy density of superconducting surface currents is given by $\frac{1}{2}\Lambda J^2 + \frac{1}{2}\mu H^2$ and many measurements of inductance and surface impedance have included this contribution to the energy. Recently, however, Little (Ref. 17) demonstrated that in a long superconducting line of very small cross section and small carrier concentration that the kinetic inductance can be made comparable to the magnetic inductance.

The present investigation stems from Little's work but the idea that electric currents should possess inertia because of the mass is very old. Faraday (Ref. 18) and Hertz (Ref. 19) both did unsuccessful experiments to try to detect it. From a modern stand-point we can understand why L_k is a very difficult quantity to measure in normal wire. The resistance of a wire is

$$R = [(m/ne^2)\cdot(l/\sigma)](1/\tau),$$

where τ is the electron collision time. On the other hand, the kinetic reactance of this same wire is

$$\omega L_k = [(m/ne^2)\cdot(l/\sigma)]\,\omega.$$

Only when $\omega > 1/\tau$ will the kinetic reactance dominate the resistance, and this frequency might be 10^{13} cycles/sec at room temperature. However, with a superconductor $\tau \rightarrow \infty$ and ωL_k can dominate R at any frequency.

Measurement technique. -- Even in superconductors L_k is not typically a large quantity. For instance, in a 1 m length of 0.25 mm diam superconducting wire well below its transition temperature $L_K \approx 10^{-10}$ H. To measure such small changes in inductance a tunnel diode oscillator circuit operating at liquid-helium temperatures has been used. This circuit (Fig. 1) was developed by Heybey (Ref. 20) and used by Boghosian et al. (Ref. 21) to measure small changes in capacitance. It was adapted to the present purpose by simply including the kinetic inductance as part of the inductance tank circuit of the oscillator. We operated in the vicinity of 15 MHz with a total inductance of about 1 μH. Since the oscillator has a short term stability of about one part in 10^7 the least count in inductance change and the frequency change (for small fractional changes) is obtained by differentiating the resonance condition

$$\omega^2 = (1/LC)\,[1 + (R^2C/L)\,], \tag{18}$$

to obtain

$$\Delta\omega/\omega_0 = -(\Delta L/2L_0)\,[\,1 - (2/Q^2)\,] - (\Delta R/R)\cdot(1/Q^2), \tag{19}$$

where $\omega_0^2 = 1/LC$. This relation shows that for reasonably high values of Q ($Q \approx 100$ and is limited by losses in the biasing circuit used) the frequency changes are proportional to the change in inductance and resistive effects can be neglected. Except very near T_c, the resistive effects could be neglected in the present measurements, a fact which was independently checked by making some of the measurements at a value of the capacitance in the tank circuit. The advantages of this technique are simplicity and sensitivity; the fact that the oscillator is located in the liquid helium and is compact is important since its allows the large bypass capacitor to reduce the effect of the cryostat and leads to a negligible value.

Experimental verification. -- To check these theoretical predictions concerning kinetic inductance calculations and measurements were made in two simple special cases, the cylindrical wire and the thin film strip of rectangular cross-section. This work has been reported in Ref. 22. The inductance of tin, indium, and aluminum wires were measured as a function of temperature and compared with the inductance calculated from the BCS theory. The measurements on tin and indium wires showed that the inductance and its temperature dependence was in reasonable agreement with that predicted for the theory. For aluminum, an extreme non-local superconductor, it was decided to attempt a precision measurement of the temperature dependence of the inductance. This experimental measurement (See Fig. 24) which is described in detail in an article to be published arrived at two essential conclusions. It found that the temperature dependence of the penetration depth as measured by this new method as shown in Fig. 25 agreed within the experimental error with previous measurements although it appeared to be considerably more sensitive. This result gives us considerable confidence that this method of calculation and measurement of inductance is valid. In addition, the experiments seem to demonstrate that the temperature dependence of aluminum does not fit the theoretically-expected temperature dependence for an extreme non-local superconductor. This conclusion and the fact that the present measurements agreed with previous temperature dependent measurements seem to show that the often quoted absolute value of 500 Å for the penetration depth of aluminum has no secure experimental basis.

Of more significance in applications was the measurement of the inductance of thin film superconducting strips of rectangular cross-section. Here a method of calculating the inductance was developed (Ref. 22) even though the current distribution is not uniform. Inductance measurements on thin films of tin in the meander-line patterns and thicknesses from 825 to 8200 Å (See Fig. 26 and Fig. 27) showed that the calculated values for kinetic inductance and their temperature dependence was well described by the theory.

Applications. -- The original purpose for studying kinetic inductnace in superconductors was to understand the behavior of thin film bridges used in flux quanti-

Fig. 24 Measurement of the change in frequency of a pure aluminum wire against the normalized BCS non-local temperature dependence $z^*(T)/Z^*(0)$.

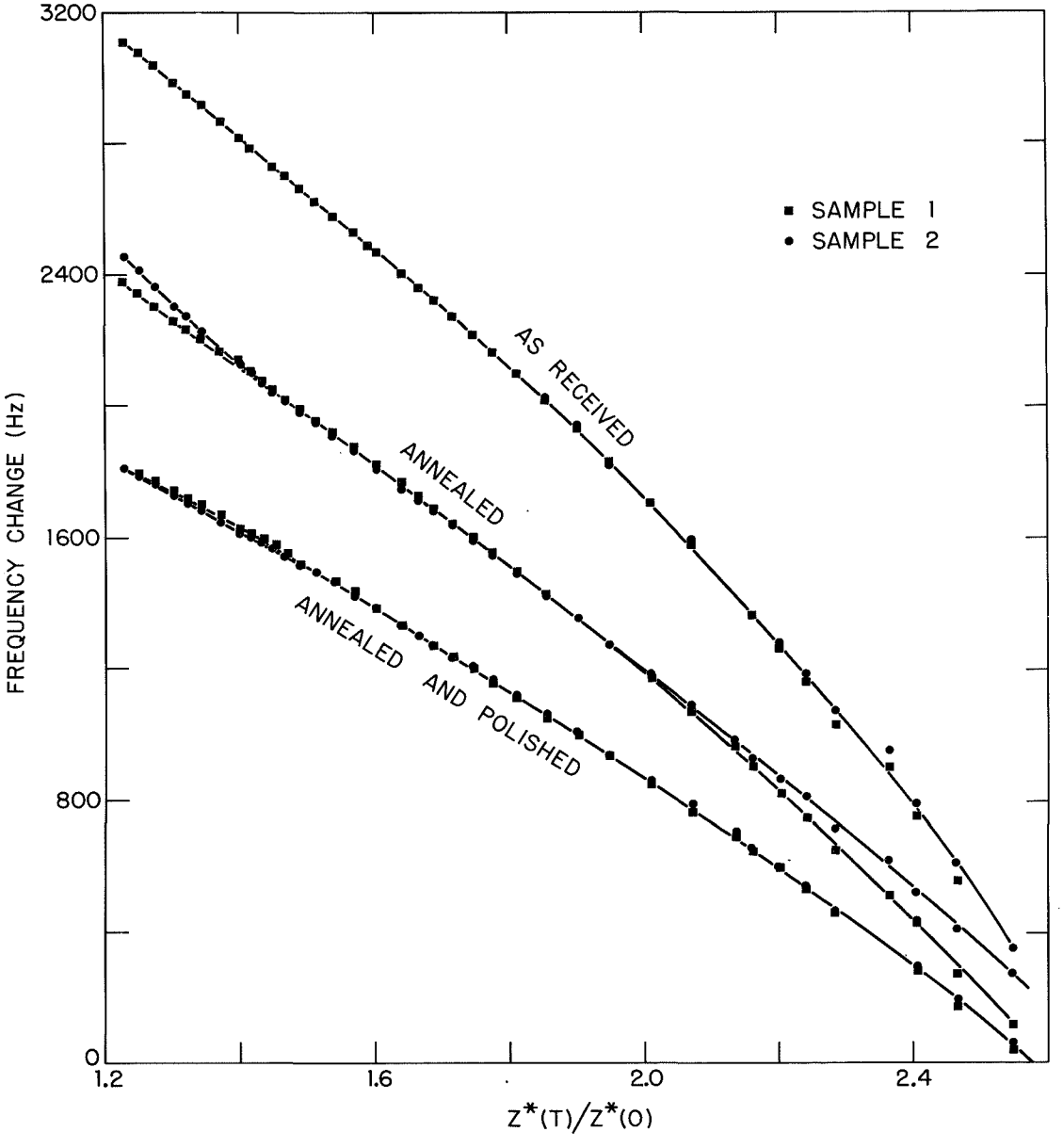

Fig. 25 $d\lambda/dy$ for aluminum from various measurements. λ = penetration depth, $y = (1 - t)^{-\frac{1}{2}}$.

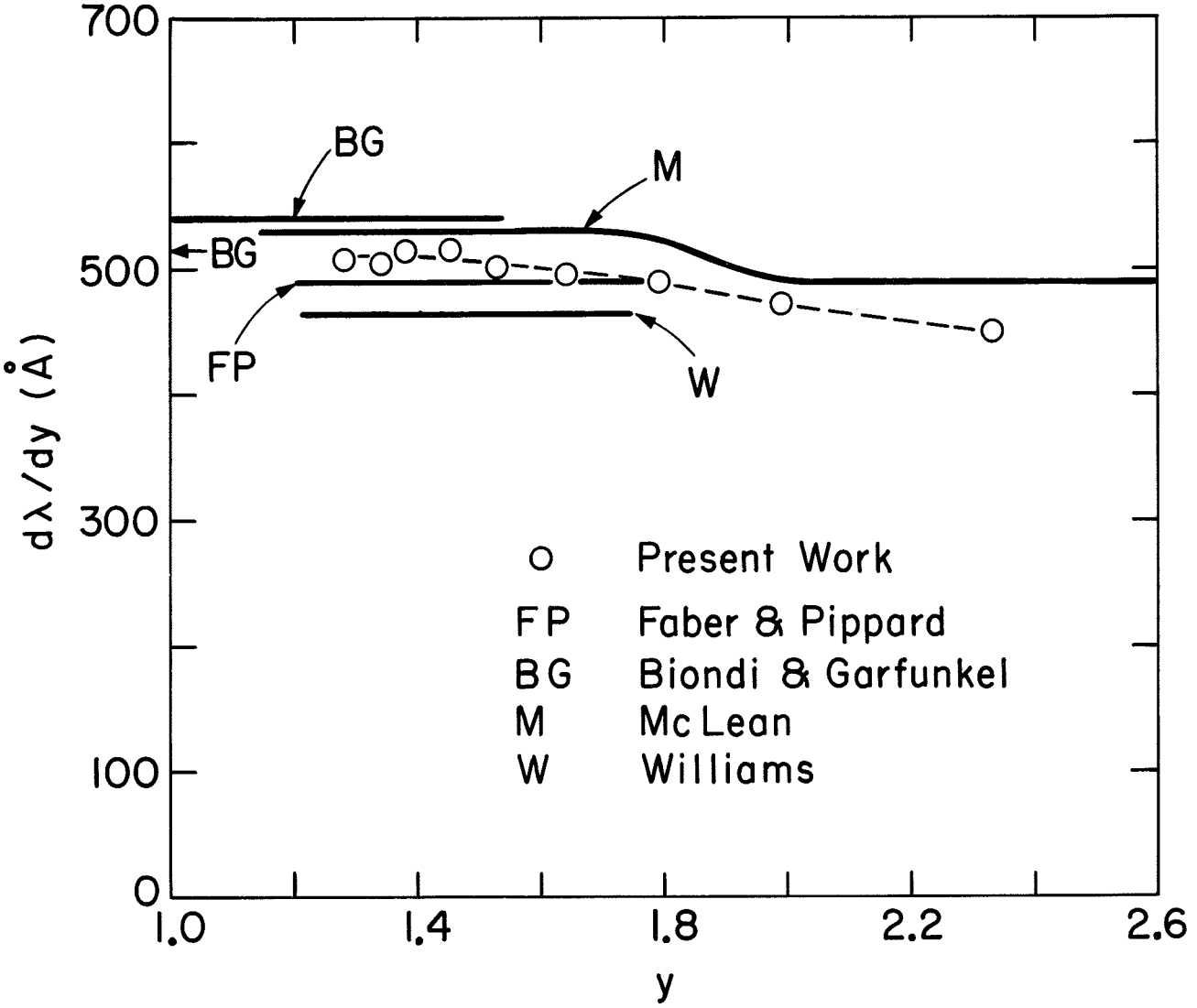

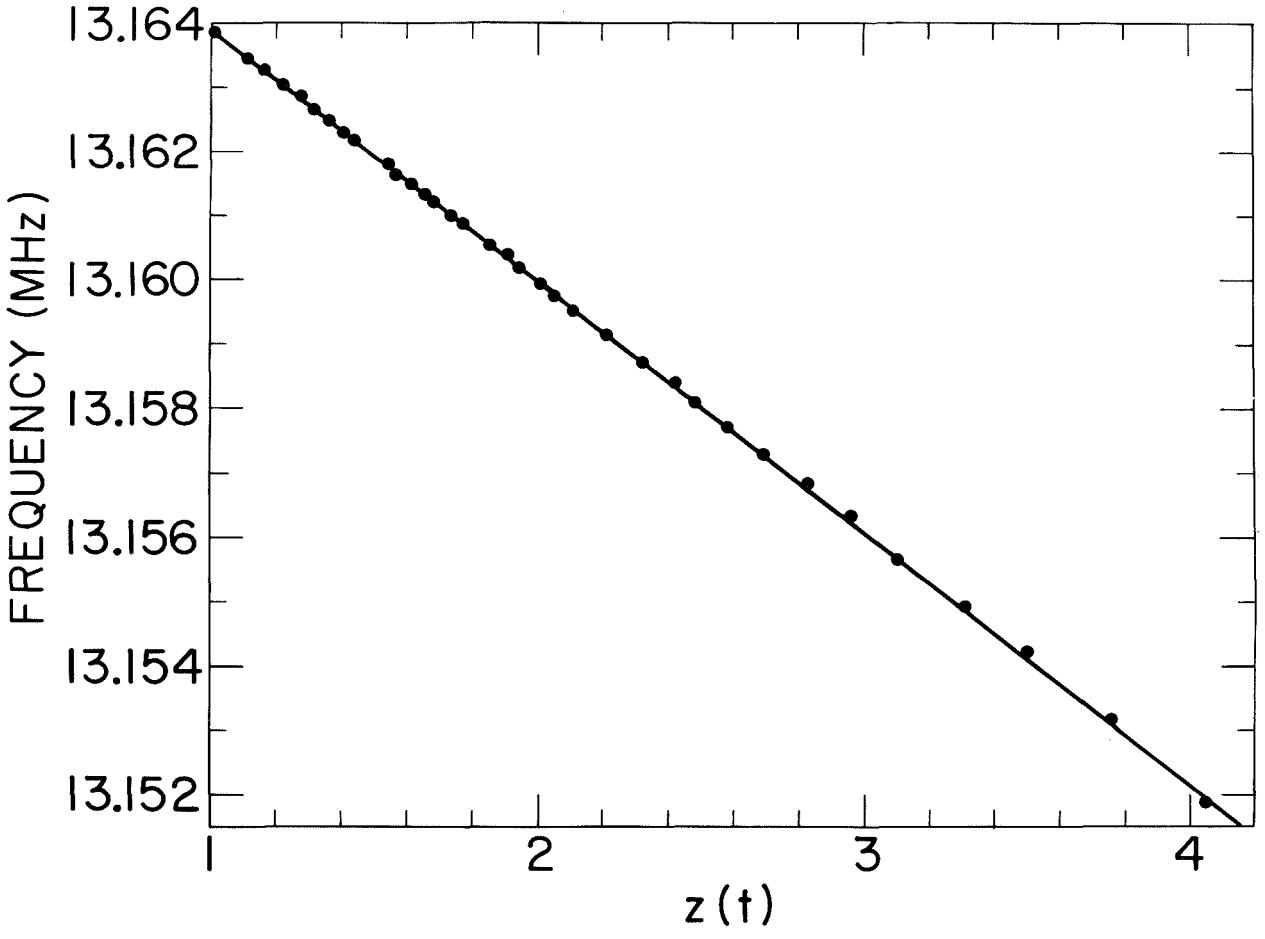

Fig. 26 Change of inductance, L, of 8200 Å tin film as a function of the BCS local temperature dependence Z(t).

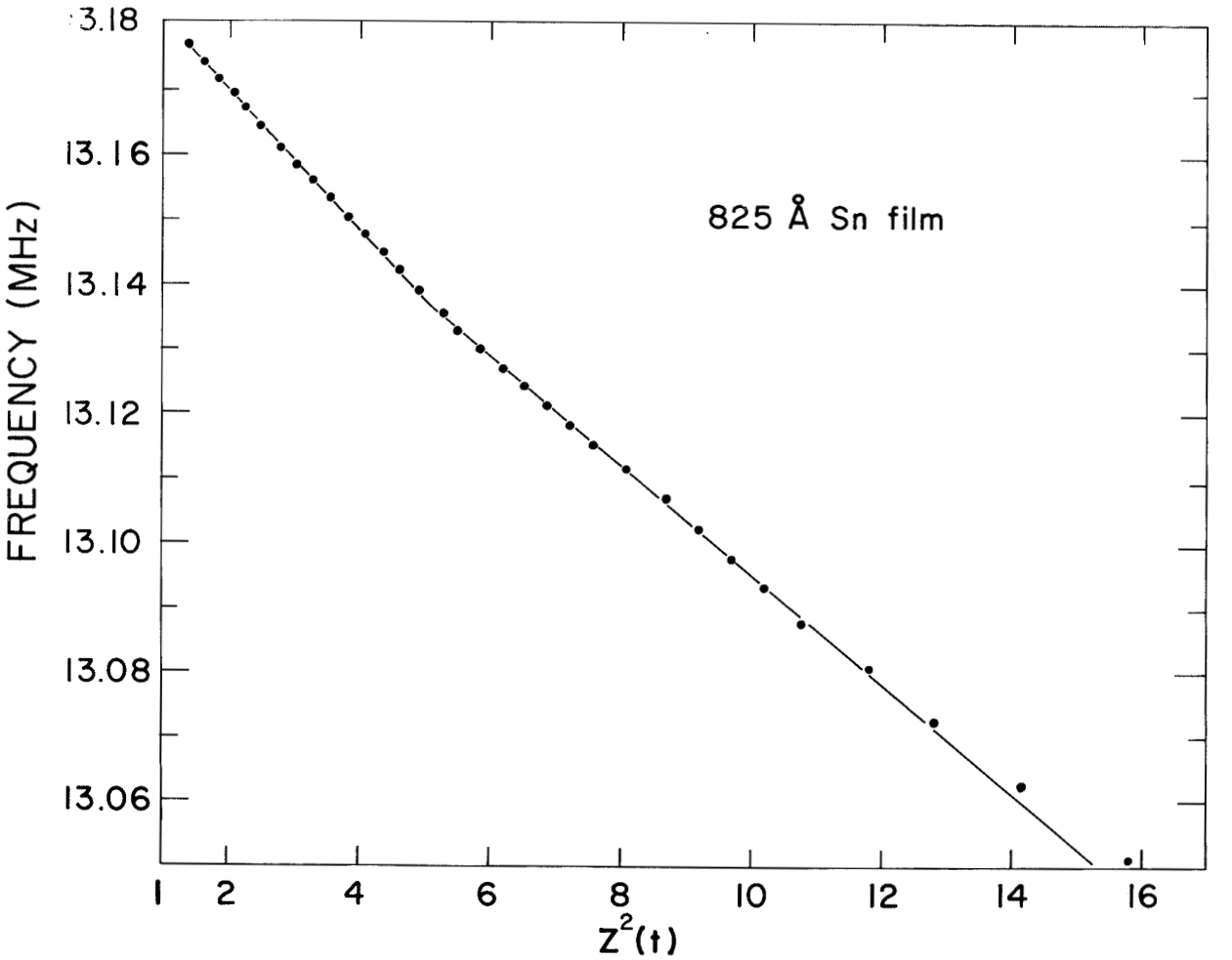

Fig. 27 L versus Z for 825 Å tin film.

zation experiments. As a result of these studies the method used in measuring the inductance turned out to be a new and very sensitive method for detecting fluxons. This method has certain unique advantages. Previously all detectors of fluxons had actually measured a resistance change in the thin film link. This required the sample be in the resistive superconducting state and therefore subject to all the erratic behavior associated with the superconducting to normal transition. By measuring the inductance rather than the resistance, it is possible to approach the superconducting to normal phase boundary where the carrier concentration is small and the sensi tivity is large and still away from the actual resistive region. Besides having certain practical advantages this method seems to eliminate a potential source of error, the fact that in the dissipative state,angular momentum may not be a good quantum number.

In addition to these applications connected with investigating the thin film links used in magnetometers and ammeters, two other possible applications became apparent during the course of the investigation. It was found that thin film superconducting meander-lines near the superconducting transition temperature gave enormous changes in frequency of the resonant circuit. These frequency changes were caused by rapid changes in the inductance and/or resistance in the meander-lines near T_c. Fig. 28 shows the frequency change for a 1000 Å thick aluminum film as a function of temperature near the transition temperature. In the region of the steepest slope a change in temperature corresponding to about 5×10^{-7} K was detectable in the counting period of one second. Since the specific heat of a 1000 Å thick aluminum is extremely small the possibility of developing a rapidly responding thermal detector seems good. By staying slightly under T_c this method of measuring the kinetic inductance avoids the large fluctuations in resistance observed in the transition region in superconducting bolometers, which have to do with fluctuations of large domains between the normal and superconducting state.

The resonant frequency was also found to be a strong function of the perpendicular magnetic field. Fig. 29 shows the measured frewuency as a function of magnetic field perpendicular to the sample as a gauss meter the oscillator had a sensitivity of about 10^{-5} gauss/Hz. The hysteresis observed was thought to be caused

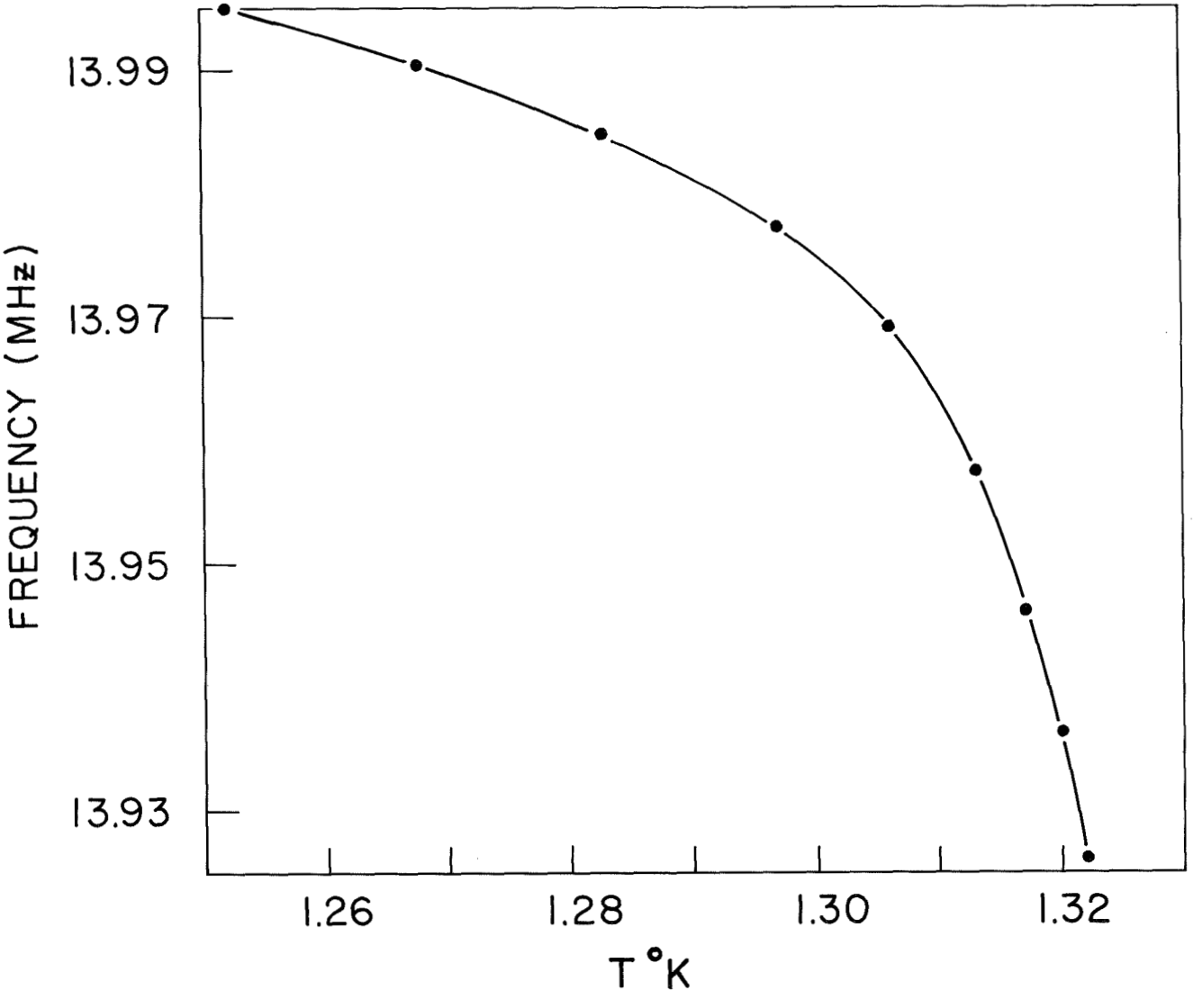

Fig. 28 Frequency versus T for 1000 Å Al film.
The sensitvity is greater than 10^{-6} K/Hz.

Fig. 29 Frequency vs. H for a 1000 Å Al film. As a gaussmeter, the sensitivity is 10^{-5} G/Hz.

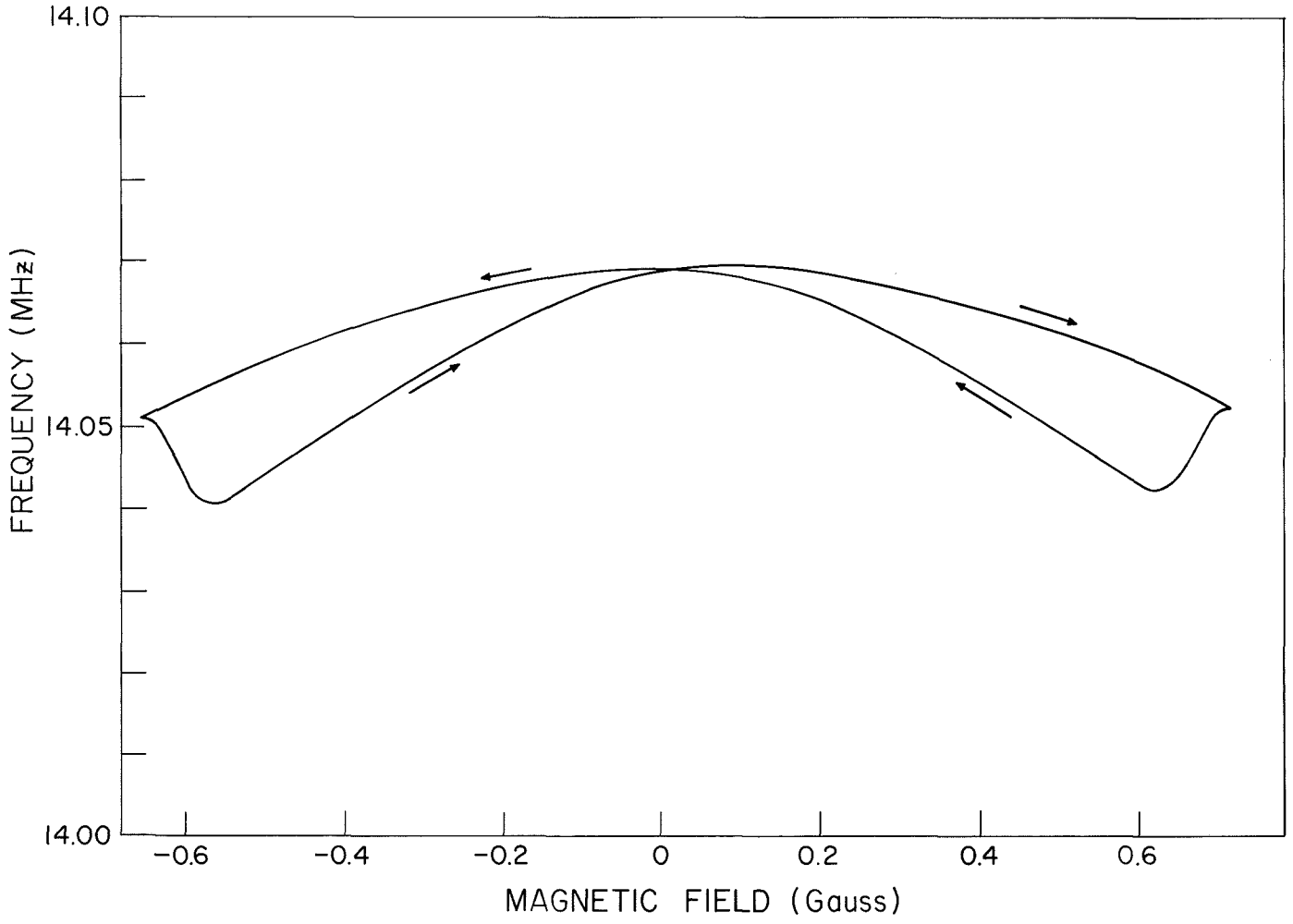

by boundary currents in the aluminum films. By making even thinner is is probable that this hysteresis could be eliminated. On the other hand, it is not certain that it would be possible to make a film thin enough so that it could be effectively operated far from the transition temperature where its temperature sensitivity would therefore not interfere with its field-measuring properties. However, it is apparent that such thin-film transducers offer a very sensitive method to detect changes in magnetic field or temperature as well as current density.

Absolute Value of the Penetration Depth

One of the goals of this research was to use flux quantization to measure magnetic penetration depths of superconductors. The technique developed by Meservey (Ref. 23) based on flux quantization is one of the only methods which actually measures the absolute value of the penetration depth. Most other methods only measure the temperature dependence of the penetration depth and rely on a theoretical expression to derive the absolute value. The penetration depth is defined as

$$\lambda \equiv \frac{1}{H_0} \int_0^\infty H \cdot dx \tag{20}$$

This characteristic length, which measures the penetration depth of the magnetic field into a superconductor is one of the two basic lengths associated with superconductivity. It is easy to see by this definition that the flux actually contained within the volume of the superconductor divided by the applied field H_0 is the penetration depth λ.

The essence of the method is to be understood from Fig. 30 and Eq. 3, which can be written as

$$\frac{m}{ne} \oint J \cdot dl + e\,\Phi = Nh \tag{3a}$$

If we pick the contour on which the current $J = 0$, then on this contour the flux Φ is quantized and we have that

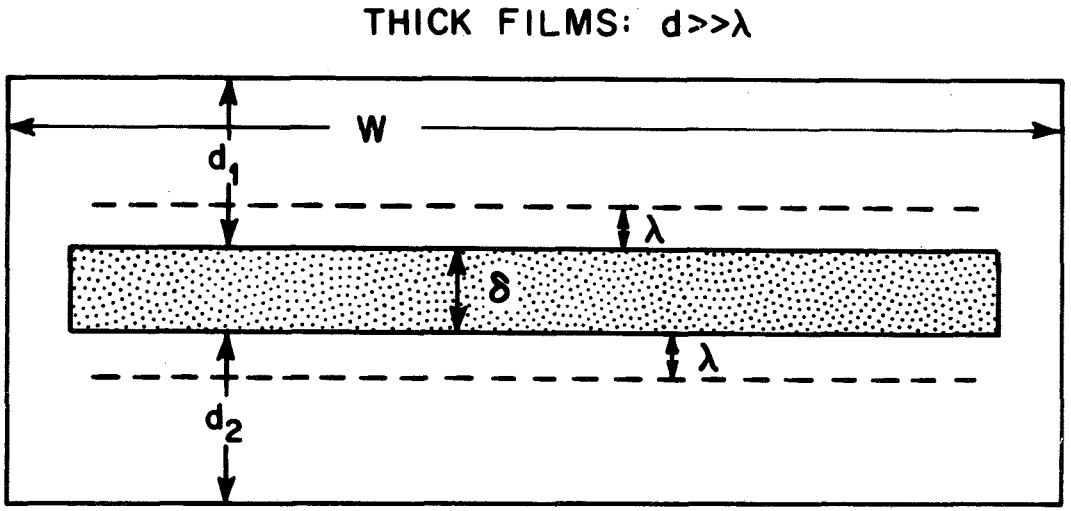

$$\phi_1 = \mu \cdot \Delta H \cdot [2\lambda + \delta] \cdot W$$

$$\lambda \equiv \frac{1}{H_0} \int_0^\infty H \, dz$$

Fig. 30 Diagram showing simplified geometry of flux quantization experiment to determine the penetration depth λ.

$$\varphi_o = \mu_o \cdot \Delta H \cdot W[\delta + 2\lambda]. \qquad (21)$$

This expression applies to sheets of a bulk superconductor where the separation of the superconductor is δ and the width between the superconducting contacts is W. ΔH is the field periodicity which is obtained by measuring the field difference between positions where the critical current of the parallel pair of superconducting junctions shown in Fig. 30 is a maximum. A simple argument shows that this position should correspond to where the current density is 0 along the centers of the superconducting sheets. When the superconducting sheets are thin films, the equivalent expression to Eq. 21 is

$$\phi_o = \mu_o \cdot \Delta H \cdot W\left(\delta + \lambda_1 \tanh \frac{d_1}{\lambda_1} + \lambda_2 \tanh \frac{d_2}{\lambda_2}\right) \qquad (22)$$

From this and the measured properties of the films we can obtain the penetration depth.

This method was applied to measuring the absolute value of the penetration depth in tin and lead films. The most difficult problem was in making the localized shorts between the two superconducting films in a place whose location was known and which had the proper conductivity. The technique which was finally evolved consisted of eight successive evaporations. These evaporations were carried out in a very high vacuum system in which the sources, masks, or substrates could be independently changed. Fig. 31 shows the sequential details of the various evaporations. Fig. 32 shows a schematic view of the thin film structure showing the essential features of the superconducting doubly-connected structure and the measuring circuit. The voltage curves for two different samples from which the magnetic field period could be measured are shown in Fig. 33. The most important results of the measurements are the absolute values of the penetration depth obtained. The result for T = 0 were for lead $\lambda_{Pb}(0) = 540 \pm 40$ Å and for tin $\lambda_{sn}(0) = 600 \pm 50$ Å. These values have been corrected for mean free path effects in the films and non-locality. The values are somewhat higher than those previously accepted, but are probably more reliable because they do not depend critically on the theoretical value of the temperature dependence of λ, as do most previous measurements. These

Fig. 31 (a) and (b). Stages in the sample evaporation. (c) Top view of completed sample. (1) Sn or Pb, (2) S:O, (3) S:O, (4) Pb, (5) Pb, (6) Pb, (7) In-Sn solder.

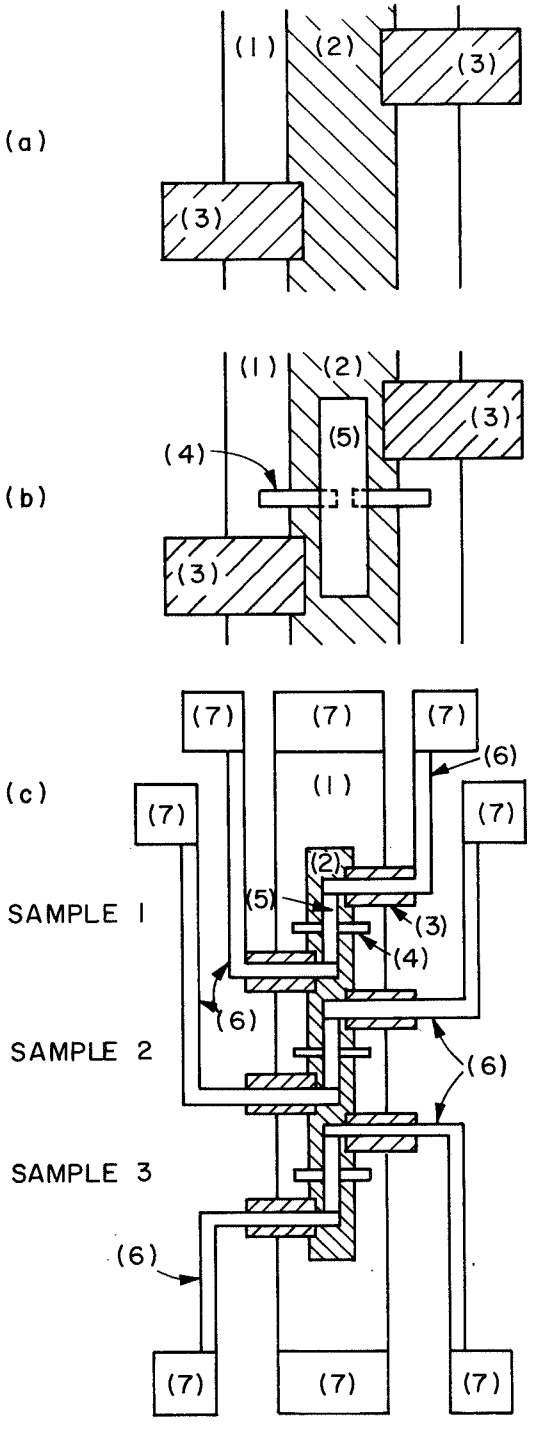

Fig. 32 End view of the sample (vertical scale much exaggeraged) and the four terminal network.

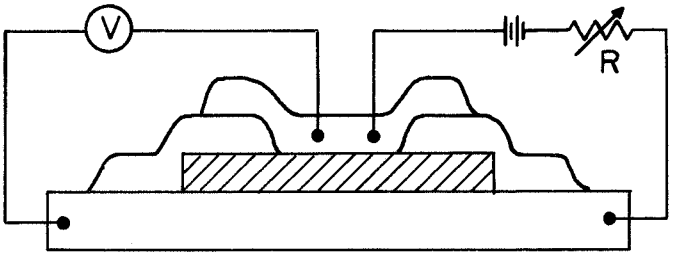

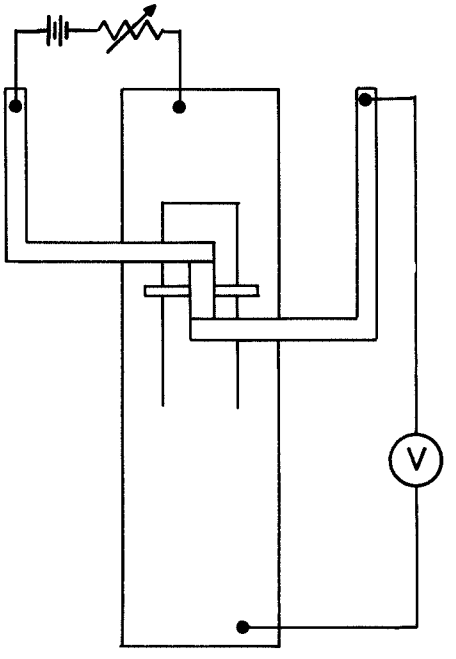

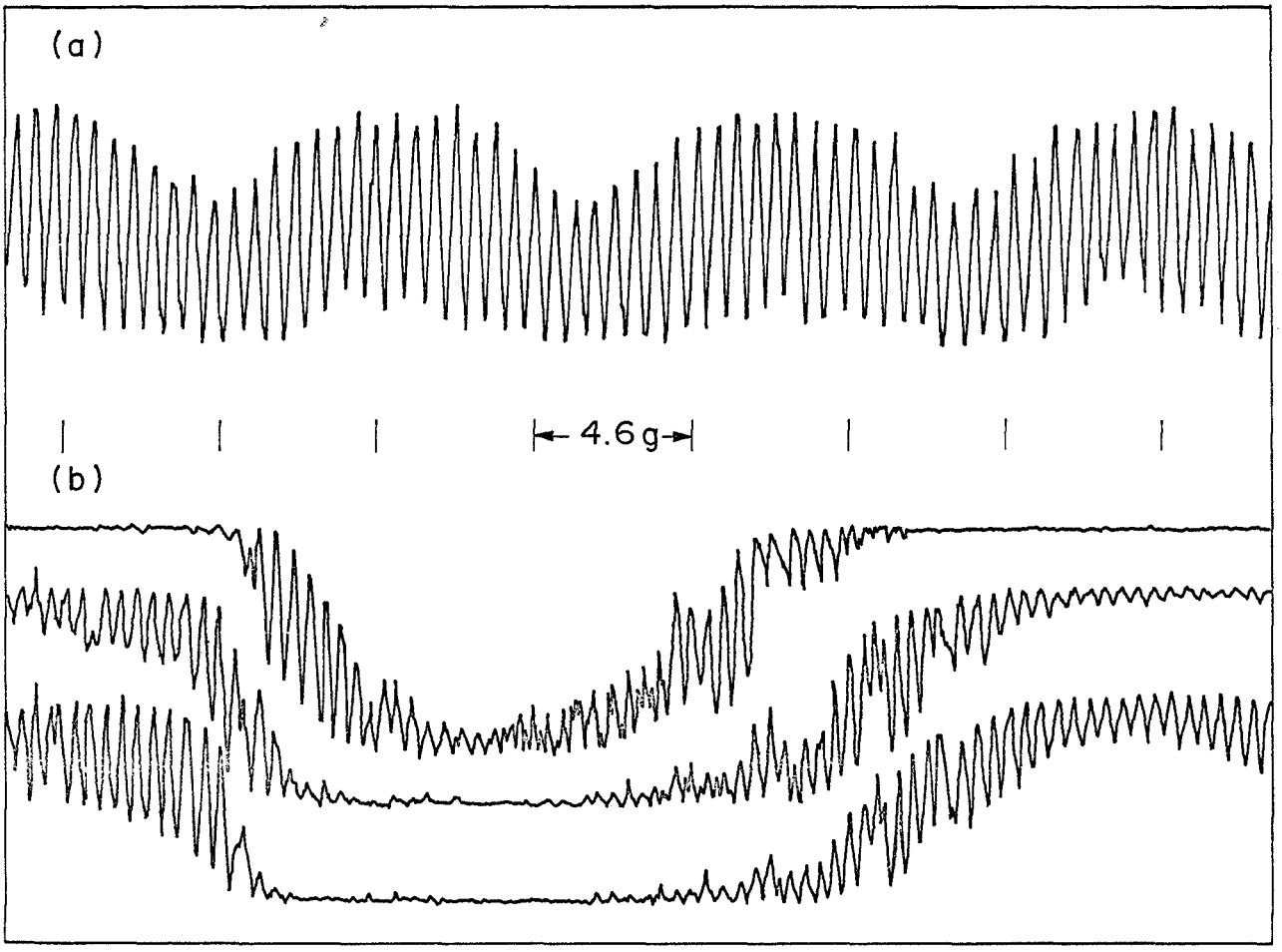

Fig. 33 Voltage-magnetic field curve for two different samples.

measurements were described in detail in Ref. 24.

Other Investigations

In addition to the research which was directly connected to the goals of this investigation, certain other results, which were a by product and seemed worthy of reporting are mentioned below.

Digital Paramagnetic Thermometer. -- In the measurements of kinetic inductance meter capable of measuring 10^{-13} henry was developed. Because of its great sensitivity at low temperature it was decided to incorporate it into a paramagnetic thermometer. A 1.0 μH copper coil was wound on a 3/8 inch quartz tube which had been filled with gadolinium sulfate and sealed. The susceptibility of the paramagnetic salt, which is a function of temperature, changes the inductance of the coil, and thus the resonant frequency of the oscillator. For small changes of susceptibility, χ , the fractional change in the resonant frequency ω is $\Delta\omega = -\chi/2$. The susceptibility of a paramagnetic salt varies with temperature very nearly as $\chi = K/T$ when not too close to the Curie temperature. Consequently for small changes

$$\Delta\omega = -\omega_o \, K/2T.$$

That is, the frequency varies as 1/T. Measurements showed that the frequency of the gadolinium sulfate thermometer (as measured on a counter) plotted against the reciprocal of the absolute temperature is very nearly, but not quite, a straight line. At least some of the deviation is to be attributed to the fact that the frequency change is so large that the frequency is no longer linear with χ. The 1/T dependence is also not exact at the lowest temperatures reached. There was a slight change in the frequency after warming to room temperature. The change is probably caused by a change of the position of the salt in the quartz container. Near 1°K it was found that a difference of about 10^{-6} °K could be detected on the counter. For much lower temperatures one could use other paramagnetic salts with lower Curie temperatures. This thermometer appears to be a very convenient device for temperature measurements over a wide range. It has been found that by encasing the paramagnetic salt in epoxy, the device can be made stable to temperature cycling

so that full advantage can be made of the digital output, thus allowing a one to one correspondence between output counts and temperature.

Microcylinder Radiation Detector. -- In the course of the measurements of microcylinders it was found that a 500 Å superconducting thin film cylinder, 0.5 microns in diameter, and 1 mm long could detect changes in power of 10^{-16} watt. Although this was not actually used as a radiation detector, such use seemed entirely feasible. The very high spatial resolution of such a detector together with its high sensitivity appeared to give unique possibilities as detectors for radiant energy and even low energy particles.

Fission Particle Technique. -- A technique was tried in which fission particles from a Californium isotope (Cf^{252}) was used to make small holes in a very thin insulating sheet. The basic idea was to make two such holes and fill them in with superconductor which would then connect the superconducting films on each side of the insulator. This would make a flux quantization loop with a very small and controllably sized hole in the size range from 25 Å to 10,000 Å. Such holes were made in very thin mica sheets which were then coated on one side with lead. Using a lead plating bath it was attempted to plate lead through the length of the hole and then to finally coat the front side of the mica with a superconductor. The technique proved successful using holes of the order of 1 micron in diameter. For practical thin links, however, the diameter should perhaps be at least 10 times smaller. Because of the fact that our technique of producing shorted thin films junctions was adequate for the flux quantization measurements of the penetration depth in superconductors, no attempt was made to develop this fission particle technique any further. However, it did appear to be a very promising technique for making superconducting bridges of very restricted cross sectional area.

CONCLUSIONS

At the start of this research it appeared that flux quantization was a very promising field of basic scientific interest and potential applications. During the period of the contract this promise has been fulfilled in a number of ways.

Of scientific interest was the study of flux quantization in thin-film micro-cylinders because of the information gained on the basic phenomenon. Also the flux quantization measurement of the penetration depth of Sn and Pb gave for perhaps the first time a directly-measured absolute value of this quantity. Finally the existence of kinetic inductance was clearly demonstrated and quantitatively measured for the first time. .

For potential applications the feasibility studies of the magnetometer and ammeter demonstrated that these instruments can be designed to have very great accuracy as well as being very sensitive. A number of possible limitations on the accuracy were studied and found to be avoidable. The technique of sensing small changes in kinetic inductance to measure small changes in magnetic field, current density, temperature, and radiation all seem to have applications in superconducting instrumentation. The very high sensitivity inductance meter developed can be used for other applications such as digital paramagnetic thermometer.

In conclusion the most important question to discuss concerns the future possible developments in flux quantization and thin film superconductivity. On the basis of the present investigation, as well as others, it seems very likely that flux quantization and its energy-time analogue, the ac Josephson effect, will come to completely dominate precision measurements of electromagnetic quantities. The development of standards is a slow process but the progress to date is very encouraging. Since most modern measurements are electromagnetic in nature, this is a very important long-term scientific development. In the measurement of very small voltages and magnetic fields, superconductors appear to have a lower threshold than other detectors. The use of Josephson junctions to produce and receive radiant energy in the far infrared appears to offer greatly improved sources and receivers in this region of the spectrum. The use of kinetic inductors with very low carrier concentration in micro-miniature thin film circuits offers transducers the possibility for measurement of small changes in magnetic field, temperature, or current density. For all of the above devices one basic, and as yet incompletely answered question concerns the noise limitation of such devices because of fluctuations in, or at the boundary of, the superconducting state. Only by a more complete understanding of these fluctuations can we

determine the ultimate limitations of flux quantization and thin film superconducting devices.

References

1. Doll, R. and Näbauer, M., Phys. Rev. Letters 7, 51 (1961).

2. Deaver, B.S., Jr. and Fairbank, W.M., Phys. Rev. Letters 7, 43 (1961).

3. London, F.: Superfluids. Vol. 1., John Wiley and Sons, Inc. 1950, p. 152.

4. Onsager, L., Procedings of the International Conference of Theoretical Physics, Kyoto and Tokyo., Science Council of Japan, Tokyo, 1954, p. 935.

5. Onsager, L., Phys. Rev. Letters, 7, 50 (1961).

6. Bardeen, J., Cooper, L.N., and Shrieffer, J.R., Phys. Rev. 108, 1175 (1957).

7. Josephson, B.D., Physics Letters 1, 251 (1962).

8. Blake, C. and Chase, C.E., Rev. Sci. Inst. 34, 984 (1963).

9. Little, W.A. and Parks, R.D., Phys. Rev. Letters 9, 9 (1962).

10. Ginzburg, V.L. and Landau, L.D., Zh. Eksperim. i Teor. Fiz. 20, 1064 (1950).

11. Tinkham, M., Phys. Rev. 129, 2413 (1963).

12. Spence, S., Thesis Stanford University (1968)
Unpublished.

13. Meservey, R. and Meyers, L., Physics Letters 26A, 367 (1968).

14. Zimmerman, J.E. and Silver, A.H., Phys. Rev. 141, 367 (1966).

15. Meservey, R., J. Appl. Phys. 39, 2598, (1968).

16. Parker, W.H., Taylor, B.N., and Langenberg, D.N., Phys. Rev. Letters 18, 287 (1967).

17. Little, W.A., Proc. of the Symposium on the Physics of Superconducting Devices, Charlottesville, Va., 1967, p. s-1.

18. Faraday, M., Experimental Researches in Electricity, (Bernard Quaritch, London, 1839), Vol. 1, p. 330.

19. Hertz, H., Miscellaneous Papers by Heinrich Hertz. English trans. D.E. Jones and G.A. Schott (MacMillan and Co. Ltd., London, 1896), pp. 1 and 137.

20. Heybey, O., Master's thesis, Cornell University (1962) (unpublished).

21. Boghosian C., Meyer, H. and Rives, J., Phys. Rev. 146, 110 (1966).

22. Meservey, R. and Tedrow, P., J. Appl. Phys. 40, 2028 (1969).

23. Meservey, R.: Low Temperature Physics - LT9 (Part A), Plenum Press, 1965, pp. 455 - 458.

24. Peabody, G.E., Ph.D. Thesis in Physics, Harvard University 1969 (unpublished). A description of this experiment is being prepared for publication.